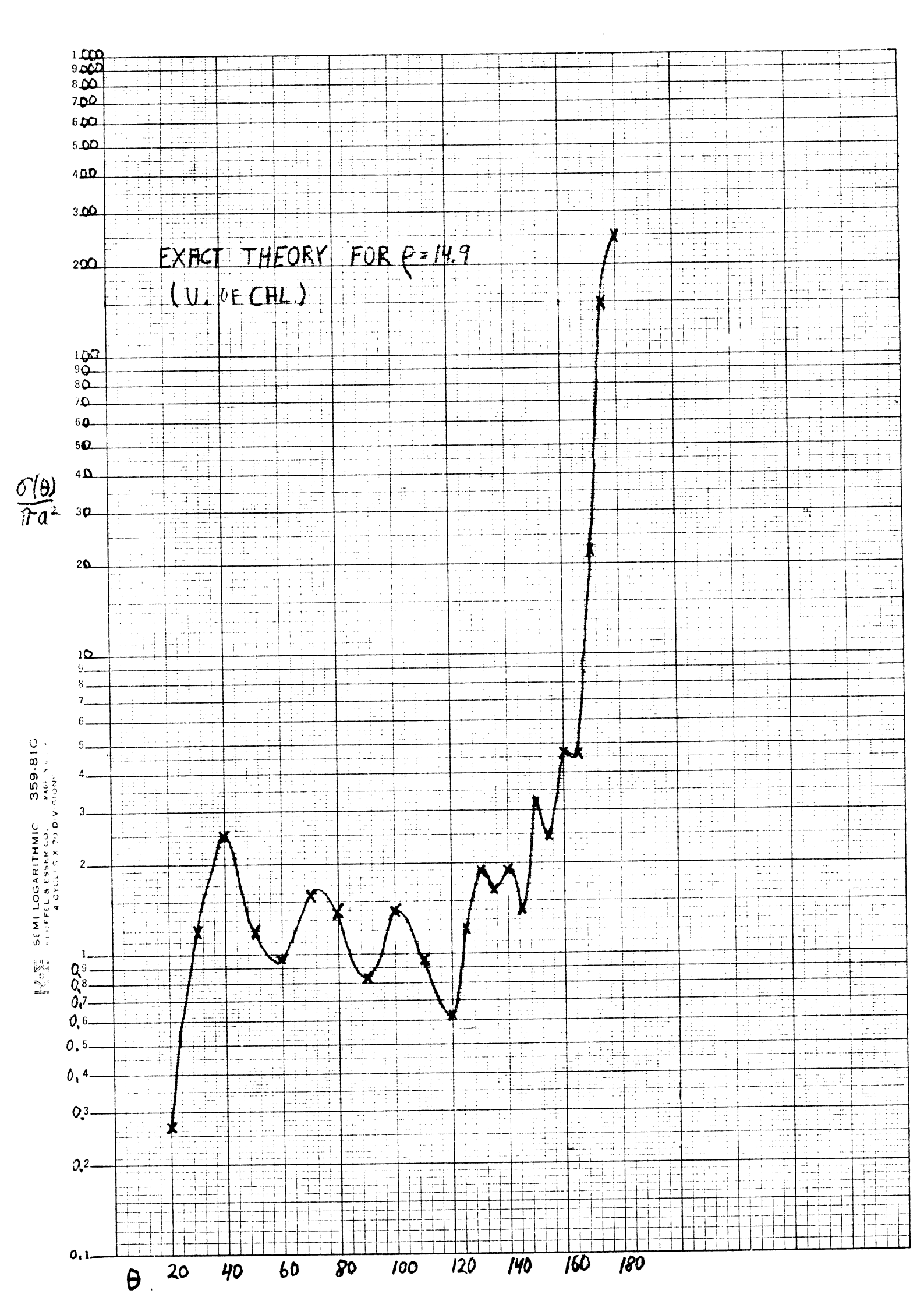
EXACT THEORY FOR ρ = 14.9
(U. OF CAL.)
σ(θ) / πa²
θ
20
40
60
80
100
120
140
160
180
1000
900
800
700
600
500
400
300
200
100
90
80
70
60
50
40
30
20
10
9
8
7
6
5
4
3
2
1
0.9
0.8
0.7
0.6
0.5
0.4
0.3
0.2
0.1
SEMI LOGARITHMIC 359-81C
KEUFFEL & ESSER CO.
4 CYCLES X 70 DIVISIONS

THE UNIVERSITY OF MICHIGAN
ENGINEERING RESEARCH INSTITUTE

TELEPHONE: NOrmandy 3-1511
ext. 3037

THE RADIATION LABORATORY

912 N. Main
Ann Arbor, Michigan

27 February 1958

Memo To All holders of "Studies in Radar Cross Sections X - Scattering of Electromagnetic Waves by Spheres (2255-20-T)" UNCLASSIFIED

Subject Corrections

I On page 40 the line ——·· —— should not appear in the legends in Figures 4 or 5. In Figure 4 the Cornell Aeronautical Laboratory's curve coincides with the National Physical Laboratory's curve as far as NPL computed, to $\rho_a > 10$ and is as shown for $\rho_a > 10$. Figure 5 is poorly drawn in comparison with the curves of the same data on Figure 4 which was fairly accurately drawn. It is useful for its purpose of showing the general trends and periodicities in the various solutions but should not be used for accurate numerical values.

II In Figure 6, page 45, the curve for $\rho = 12.8$ is incorrectly attributed to Hamren (exact theory, Univ of Calif). However, it was actually obtained at The University of Michigan. Hamren's curve is really for $\rho = 14.9$, and was inadvertently omitted from Figure 6. We give his results below, converted to $\sigma(\theta)/\pi a^2$ versus θ as variables.

III The third and eleventh lines of page 34 exhibit a typographical error, resulting in a misrepresentation of Franz's words. They should read "running from P_1 or P_2 respectively" rather than "running from P_1 to P_2". The validity of the subsequent criticism is still a point of contention between Dr. Kaplan and Dr. Franz, concerning which we reserve judgement.

IV There are errors in Equations 5 - 20, page 67. These should read

$$\left.\begin{aligned} \frac{2n+3}{(n+1)(n+2)} X_{n+1} + \frac{n}{n+1} Y_n - \frac{n+3}{n+2} Y_{n+2} &= 0 \\ \frac{2n+3}{(n+1)(n+2)} Y_{n+1} + \frac{n}{n+1} X_n - \frac{n+3}{n+2} X_{n+2} &= 0 \end{aligned}\right\}$$

The stated conclusions now follow properly from the equations.

M. L. Barasch

H. Weil

jr

2255-20-T

Studies in Radar Cross-Sections-X

Scattering of Electromagnetic Waves by Spheres

H. Weil, M. L. Barasch, and T. A. Kaplan

Work Performed for
Rome Air Development Center,
Contract AF 30(602)-1070

July 1956

The University of Michigan
Engineering Research Institute
Willow Run Laboratories
Willow Run Airport
Ypsilanti, Michigan

STUDIES IN RADAR CROSS-SECTIONS

The University of Michigan
Engineering Research Institute

I Scattering by a Prolate Spheroid, F. V. Schultz (UMM-42, March 1950), Contract W-33(038)-ac-14222, UNCLASSIFIED.

II The Zeros of the Associated Legendre Functions $P_n^m(\mu')$ of Non-Integral Degree, K. M. Siegel, D. M. Brown, H. E. Hunter, H. A. Alperin, and C. W. Quillen (UMM-82, April 1951) Contract W-33(038)-ac-14222, UNCLASSIFIED.

III Scattering by a Cone, K. M. Siegel and H. A. Alperin (UMM-87, January 1952), Contract AF-30(602)-9, UNCLASSIFIED.

IV Comparison Between Theory and Experiment of the Cross-Section of a Cone, K. M. Siegel, H. A. Alperin, J. W. Crispin, Jr., H. E. Hunter, R. E. Kleinman, W. C. Orthwein, and C. E. Schensted (UMM-92, February 1953), Contract AF-30(602)-9, UNCLASSIFIED.

V An Examination of Bistatic Early Warning Radars, K. M. Siegel (UMM-98, August 1952), Contract W-33(038)-ac-14222, SECRET.

VI Cross-Sections of Corner Reflectors and Other Multiple Scatters at Microwave Frequencies, R. R. Bonkowski, C. R. Lubitz, and C. E. Schensted (UMM-106, October 1953), Contract AF-30(602)-9, SECRET - UNCLASSIFIED when Appendix is removed.

VII Summary of Radar Cross-Section Studies Under Project Wizard, K. M. Siegel, J. W. Crispin, Jr., and R. E. Kleinman (UMM-108, November 1952) Contract W-33(038)-ac-14222, SECRET.

VIII Theoretical Cross-Section as a Function of Separation Angle Between Transmitter and Receiver at Small Wavelengths, K. M. Siegel, H. A. Alperin, R. R. Bonkowski, J. W. Crispin, Jr., A. L. Maffett, C. E. Schensted, and I. V. Schensted (UMM-115, October 1953), Contract W-33(038)-ac-14222, UNCLASSIFIED.

IX Electromagnetic Scattering by an Oblate Spheroid, L. M. Rauch (UMM-116, October 1953), Contract AF-30(602)-9, UNCLASSIFIED.

X Scattering of Electromagnetic Waves by Spheres, H. Weil, M. L. Barasch, and T. A. Kaplan (2255-20-T, July 1956), Contract AF 30(602)-1070, UNCLASSIFIED.

XI The Numerical Determination of the Radar Cross-Section of a Prolate Spheroid, K. M. Siegel, B. H. Gere, I. Marx and F. B. Sleator (UMM-126, December 1953), Contract AF-30(602)-9, UNCLASSIFIED.

XII Summary of Radar Cross-Section Studies Under Project MIRO, K. M. Siegel, M. E. Anderson, R. R. Bonkowski and W. C. Orthwein (UMM-127, December 1953), Contract AF-30(602)-9, SECRET.

XIII Description of a Dynamic Measurement Program, K. M. Siegel and J. M. Wolf, (UMM-128, May 1954), Contract W-33(038)-ac-14222, CONFIDENTIAL.

XIV Radar Cross-Section of a Ballistic Missile, K. M. Siegel, M. L. Barasch, J. W. Crispin, Jr., W. C. Orthwein, I. V. Schensted and H. Weil (UMM-134, September 1954), Contract W-33(038)-ac-14222, SECRET.

XV Radar Cross-Sections of B-47 and B-52 Aircraft, C. E. Schensted, J. W. Crispin, Jr., and K. M. Siegel (2260-1-T, August 1954), Contract AF-33(616)-2531, CONFIDENTIAL.

XVI Microwave Reflection Characteristics of Buildings, H. Weil, R. R. Bonkowski, T. A. Kaplan and M. Leichter (2255-12-T, May 1955), Contract AF-30(602)-1070, SECRET.

XVII Complete Scattering Matrices and Circular Polarization Cross-Sections for the B-47 Aircraft at S-Band, A. L. Maffett, M. L. Barasch, W. E. Burdick, R. F. Goodrich, W. C. Orthwein, C. E. Schensted, and K. M. Siegel (2260-6-T, June 1955), Contract AF-33(616)-2531, CONFIDENTIAL.

XVIII Airborne Passive Measures and Countermeasures, K. M. Siegel, M. L. Barasch, J. W. Crispin, Jr., R. F. Goodrich, A. H. Halpin, A. L. Maffett, W. C. Orthwein, C. E. Schensted and C. J. Titus (2260-29-F, January 1956), Contract AF-33(616)-2531, SECRET.

XIX Radar Cross-Section of a Ballistic Missile II, K. M. Siegel, M. L. Barasch, H. Brysk, J. W. Crispin, Jr., T. B. Curtz, and T. A. Kaplan (2428-3-T, January 1956), Contract AF-04(645)-33, SECRET.

XX Radar Cross-Section of Aircraft and Missiles, K. M. Siegel, W. E. Burdick, J. W. Crispin, Jr., and S. Chapman (WR-31-J, 1 March 1956), SECRET.

PREFACE

This paper is the tenth in a series of reports growing out of Studies in Radar Cross-Sections at the Engineering Research Institute of The University of Michigan. The primary aims of this program are:

1. To show that radar cross-sections can be determined analytically.
2. To elaborate means for computing cross-sections of objects of military interest.
3. To demonstrate that these theoretical cross-sections are in agreement with experimentally determined values.

Intermediate objectives are:

1. To compute the exact theoretical cross-sections of various simple bodies by solution of the appropriate boundary-value problems arising from Maxwell's equations.
2. To examine the various approximations possible in this problem, and determine the limits of their validity and utility.
3. To find means of combining the simple body solutions in order to determine the cross-sections of composite bodies.
4. To tabulate various formulas and functions necessary to enable such computations to be done quickly for arbitrary objects.
5. To collect, summarize, and evaluate existing experimental data.

Titles of the papers already published or presently in process of publication are listed on the preceding pages.

K. M. Siegel

TABLE OF CONTENTS

LIST OF FIGURES

ABSTRACT

A survey is presented of the theoretical, computational, and experimental results in the extensive literature dealing with the scattering of electromagnetic energy by spheres. Some of the main theoretical results are discussed critically and interrelated.

New theoretical and numerical results obtained at The University of Michigan supplement the survey.*

* This report was prepared by the Engineering Research Institute of The University of Michigan under Air Force Contract No. AF30(602)-1070. Work called for under this contract was performed for the Electronic Warfare Laboratory of Rome Air Development Center.

I

INTRODUCTION

The most intensively studied electromagnetic scattering problem is that of scattering from a spherical obstacle. The reasons for this interest are several. From a theoretical standpoint, the sphere is one of the few bodies for which an exact analytic solution to Maxwell's equations is available. In fact an exact solution for a perfectly conducting sphere and a plane incident wave was given as far back as 1893 by J. J. Thomson (Ref. 63). For an arbitrary sphere material the solution was given in 1908 by Mie (Ref. 41). However, the series obtained by relatively straightforward methods are very slowly convergent for spheres whose radii greatly exceed the wavelength of the incident radiation. The same remark holds for the case where the incident field is caused by a source at a finite distance from the sphere. The problem of obtaining a rapidly convergent series solution has interested many workers, as have the search for methods for obtaining approximate answers, investigations of the validity of the approximate results, and the search for physical understanding of the solutions. While much progress has been made on these interrelated problems, there are still many unanswered questions, particularly in the physical interpretation of the mathematical results.

Considerable attention has also been given to applying the theory to scattering by large numbers of spherical scatterers, thought of as representing both the individual molecules and larger scatterers

(such as dust or raindrops) in the atmosphere, or as representing the particles in colloidal solutions. Although the shapes of these scatterers are not necessarily spherical, very useful results have been obtained. Because of these important applications of the theory extensive numerical computations based on the Mie series have been carried out without waiting for the theoreticians to derive more rapidly converging series useful for computations in the range of sphere-radius-to-wavelength-ratios of interest.

For the case of a radial dipole near the sphere's surface, computationally useful rapidly converging series are available and have been used for computations of the field of a transmitter near the earth.

The principal purposes of this report are to summarize and discuss some of the main results along the above lines, interrelating and supplementing the theoretical analyses, and to discuss experimental scattering work involving spheres. Some unpublished numerical results obtained by The University of Michigan are also included.

The literature is so extensive that, as regards much of it, this report will be no more than a guide bringing various papers to the attention of the reader, and much of it will simply not be mentioned.* Detail generally will be given only in connection with a perfectly conducting sphere irradiated by a tangential dipole or a plane wave, and in particular for results which are not in the literature.

---

* See, for example, a survey article on diffraction theory by Bouwkamp (Ref. 8) which gives many references not mentioned in this report.

II

THEORETICAL RESULTS AND PHYSICAL DISCUSSIONS

2.1 INTRODUCTION

In this section the analytical results are collected, their discoverers acknowledged and their use discussed. Various methods of derivation and related theoretical questions are described and discussed in some detail in Section V.

As in all electromagnetic scattering problems the quantities computed are often the electromagnetic fields, $\vec{E}$ and $\vec{H}$, or the parts of the fields scattered by the object, $\vec{E}^S$ and $\vec{H}^S$. Very commonly it is not the scattered fields themselves but measures of their intensities and polarization or measures of the total amount of power scattered in all directions which are determined. These quantities are the various cross-sections.

The cross-sections of most common interest are the radar and total cross-sections. These assume that the incident radiation takes the form of a plane wave. The radar cross-section is defined as

$$\sigma = \lim_{r \to \infty} 4\pi r^2 \frac{\left| \vec{E}^S_{rec.} \right|^2}{\left| \vec{E}^i \right|^2}$$

where r is the distance from the scatterer to receiver, and $\vec{E}^S_{rec}$ is the scattered field at the receiver. The total cross-section is the integral of σ over the surface of a unit sphere.

The form given above has direct application when the receiver polarization is identical with that of the scattered field. When this is not the case the component of the scattered field in the direction of receiver polarization must be used for an effective cross-section.

For a more general treatment of polarization there is a 2 x 2 matrix of cross-sections corresponding to transmitting each of two orthogonal polarizations and receiving with a receiver of the same polarization as the transmitter or the orthogonal polarization. It is to be noted that whenever the incident polarization is not specified in the literature a linearly polarized wave is assumed. For more details on the treatment of polarization one can see, for example, Reference 52 or Reference 34.

2.2 THE MIE SOLUTION

Mie's (Ref. 41) widely known solution to the problem of scattering of incident plane waves by a sphere of arbitrary material is derived and discussed by Stratton (Ref. 60) and Kerr (Ref. 36). The results are also derived and alternate derivations discussed in Section V. To express the results, introduce a spherical coordinate system (r,θ,ϕ) with origin located at the center of the sphere. The system is oriented so that the incident periodic plane wave is directed along the line $\theta = 0$ in the direction of decreasing r with the electric vector in the plane $\phi = 0$. Let the sphere radius be a, the amplitude of the incident wave be E_o and its frequency be $\omega/2\pi$.

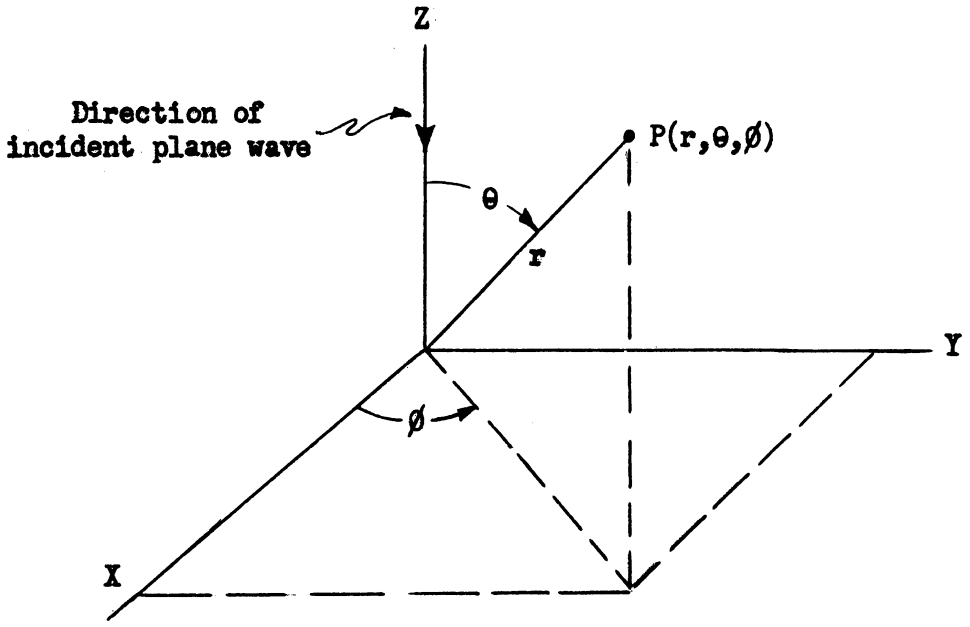

FIG. 1 COORDINATE SYSTEM

Then the components of the scattered electric field in the direction of increasing θ and ϕ are respectively

$$E_\theta^s = E_o \cos\phi\, e^{-i\omega t} \frac{1}{\rho} \sum_{n=1}^{\infty} (-i)^n \frac{2n+1}{n(n+1)} \left[a_n(\rho_a) \frac{P_n^1(\cos\theta)}{\sin\theta} \zeta_n(\rho) \right. \tag{2-1}$$

$$\left. + i\, b_n(\rho_a) \frac{dP_n^1(\cos\theta)}{d\theta} \frac{d\,\zeta_n(\rho)}{d\rho} \right] ,$$

$$E_{\phi}^{s} = -E_{o}\sin\phi\, e^{-i\omega t} \frac{1}{\rho} \sum_{n=1}^{\infty} (-i)^{n} \frac{2n+1}{n(n+1)} \left[a_n(\rho_a) \frac{d P_n^1(\cos\theta)}{d\theta} \zeta_n(\rho) \right.$$

$$\left. + i\, b_n(\rho_a) \frac{P_n^1(\cos\theta)}{\sin\theta} \frac{d\zeta_n(\rho)}{d\rho} \right] . \qquad (2\text{-}1)$$

Here k = the propagation constant in free space = $2\pi/\lambda$, ηk = propagation constant in the sphere, $\rho_a = ka$, $\rho = kr$ and μ_1 and μ_2 the magnetic permeabilities for the sphere and free space, respectively.

$$a_n = -\left[\frac{\mu_1 \psi_n(\eta\rho)\psi_n'(\rho) - \eta\mu_2 \psi_n(\rho)\psi_n'(\eta\rho)}{\mu_1 \psi_n(\eta\rho)\zeta_n'(\rho) - \eta\mu_2 \zeta_n(\rho)\psi_n'(\eta\rho)} \right]_{\rho=\rho_a}$$

$$b_n = -\left[\frac{\mu_1 \psi_n(\rho)\psi_n'(\eta\rho) - \eta\mu_2 \psi_n(\eta\rho)\psi_n'(\rho)}{\mu_1 \zeta_n(\rho)\psi_n'(\eta\rho) - \eta\mu_2 \psi_n(\eta\rho)\zeta_n'(\rho)} \right]_{\rho=\rho_a}$$

For spheres of conductivity or dielectric constant so large that $|\eta\rho_a| \gg 1$

$$a_n \cong -\frac{\psi_n(\rho_a)}{\zeta_n(\rho_a)} \quad , \quad b_n \cong -\frac{\psi_n'(\rho_a)}{\zeta_n'(\rho_a)} \quad .$$

Here prime denotes differentiation with respect to the argument. ψ_n and ζ_n are given by $\psi_\nu(x) = \sqrt{\frac{\pi x}{2}}\, J_{\nu+\frac{1}{2}}(x)$, $\zeta(x) = \sqrt{\frac{\pi x}{2}}\, H^{(1)}_{\nu+\frac{1}{2}}(x)$, and $P_n^1(\cos\theta)$ is an associated Legendre function:

$$P_n^1(\cos\theta) = -\sin\theta\, dP_n(\cos\theta)/d(\cos\theta).$$

It will be shown in Section V that these series can be very closely approximated by finite series consisting of the first N terms of Equation (2-1) where N is independent of ρ and somewhat greater than ρ_a, as shown on Figure 10.* To get a "far zone" result it is then permissible in the finite series to replace the functions $\zeta_n(\rho)$ by the asymptotic form valid for $\rho >> n^2$:

$$\zeta_n(\rho) \sim (-i)^{n+1} e^{i\rho}.^{**} \qquad (2\text{-}2)$$

These substitutions result in the following expressions for E_θ^s and E_ϕ^s:

---

* Figure 10 shows N vs ρ_a where N is large enough to insure at least 4% accuracy in evaluating the series when using only N terms.

** The justification of the use of Equation (2-2) in Equation (2-1) is generally not considered specifically in the sphere literature, although Debye (Ref. 16) states that the justification is given in his thesis (on which Reference 16 is based).

$$E_\theta^s = \frac{-iE_o \cos\phi}{\rho} e^{-i(\omega t-\rho)} \sum_{n=1}^{N} (-1)^n \frac{2n+1}{n(n+1)} \left[a_n(\rho_a) \frac{P_n^1(\cos\theta)}{\sin\theta} - b_n(\rho_a) \frac{d P_n^1(\cos\theta)}{d\theta} \right]$$

$$E_\phi^s = \frac{iE_o \sin\phi}{\rho} e^{-i(\omega t-\rho)} \sum_{n=1}^{N} (-1)^n \frac{2n+1}{n(n+1)} \left[a_n(\rho_a) \frac{dP_n^1(\cos\theta)}{d\theta} - b_n(\rho_a) \frac{P_n^1(\cos\theta)}{\sin\theta} \right] \quad (2\text{-}3)$$

Before the advent of these series solutions for spheres of arbitrary size Lord Rayleigh developed expressions for the radiation scattered by spheres small compared to wavelength. The resulting cross-sections may be obtained from the Mie series (2-3) by employing the power series expansion of the Bessel functions involved. One then sees that for spheres of finite $|\eta|$ for which $\mu_2 \sim \mu_1$ and ρ_a and $\eta\rho_a << 1$ the electric dipole radiation* dominates. Computing the cross-section from the resulting expression for the scattered field, one finally obtains

*i.e., the term with coefficient b_1; the term with coefficient a_1 will be referred to as magnetic dipole radiation.

$$\frac{64\pi^5 a^6}{\lambda^4}\left(\frac{\eta^2-1}{\eta^2+2}\right)^2\left[\cos^2\phi\cos^2\theta+\sin^2\phi\right]$$

the Rayleigh scattering cross-section for very small dielectric spheres of finite dielectric constant.

If, however, the dielectric constant, conductivity, or both, be taken as infinite, the magnetic dipole coefficient becomes half as large as that for the electric dipole, and must be included. Interference terms are now present, and the result is

$$\frac{16\pi^5 a^6}{\lambda^4}\left[(1+2\cos\theta)^2\cos^2\phi+(2+\cos\theta)^2\sin^2\phi\right]$$

It may be noted that for backscattering ($\theta=0$), the latter result is 9/4 the limit of the former one.

2.3 SOURCE AT A FINITE DISTANCE

The situation where the source is at a finite distance from the sphere is commonly used as a model for an antenna near the earth's surface. Furthermore, the situation where a plane wave is incident on the sphere is a special case of the situation where the source of the incident wave is a horizontal electric dipole, that is, a dipole oriented normal to a radial line from the sphere's center. As such a dipole recedes toward infinity the incident wave approximates a plane wave so

that the solution to this problem can be used to estimate the effect of lack of planeness in the incident wave.

An exact expression for the field arising from a horizontal dipole is obtained by Tai (Ref. 61), using relations derived by him relating radial and linear Hertzian potentials (see Section 5.1), and again by Tai (Ref. 62) and by Felsen (Ref. 17) using the general theory of tensor Green's functions.

The incident field for a dipole moment $p\hat{X}^*$ at $r = b$, $\theta = 0$ is

$\vec{E}^i = \text{curl curl} \dfrac{p\, e^{ikr_b}}{4\pi\epsilon\, r_b} p\hat{X}$, or in components,

$$E^i_\theta = \frac{p\cos\phi}{4\pi\epsilon}\,\frac{k^3}{\beta^3}\left\{(-i\beta + 1 - \beta^2)\cos\theta + (3i\beta + 3 - \beta^2)(\sin\theta\cos\theta - \cos\theta - \frac{\rho_b}{\rho}) \cdot \frac{\rho^2\sin\theta}{\beta}\right\} \qquad (2\text{-}4)$$

and

$$E^i_\phi = \frac{p\sin\phi}{4\pi\epsilon} \cdot \frac{k^3}{\beta^3}(-i\beta + 1 - \beta^2),$$

where β/k is the distance from the dipole to the point of observation.

*$\hat{X}$, $\hat{Y}$, and $\hat{Z}$ are unit vectors along the X, Y, and Z axes.

The incident field (Eq. 2-4) may be expressed as

$$E_\theta^{(inc)} = \frac{i k^3 p \cos\phi}{4\pi\epsilon\rho\rho_b} \sum_{n=1}^{\infty} \frac{2n+1}{n(n+1)} \left\{ \frac{P_n^1(\cos\theta)}{\sin\theta} \psi_n(\rho)\zeta_n(\rho_b) + \frac{\partial P_n^1(\cos\theta)}{\partial\theta} \zeta_n'(\rho_b)\psi_n'(\rho) \right\} \qquad (2\text{-}5)$$

$$E_\phi^{(inc)} = \frac{-i k^3 p \sin\phi}{4\pi\epsilon\rho\rho_b} \sum_{n=1}^{\infty} \frac{2n+1}{n(n+1)}$$

$$\times \left\{ \frac{\partial P_n^1(\cos\theta)}{\partial\theta} \zeta_n(\rho_b)\psi_n(\rho) + \frac{P_n^1(\cos\theta)}{\sin\theta} \zeta_n'(\rho_b)\psi_n'(\rho) \right\}$$

and the scattered field is

$$E_\theta^s = \frac{ik^3 p \cos\phi}{4\pi\epsilon\rho\rho_b} \sum_{n=1}^{\infty} \frac{2n+1}{n(n+1)} \left\{ \frac{P_n^1(\cos\theta)}{\sin\theta} \zeta_n(\rho_b)\zeta_n(\rho) a_n(\rho_a) + \frac{\partial P_n^1(\cos\theta)}{\partial\theta} \zeta_n'(\rho_b)\zeta_n'(\rho) b_n(\rho_a) \right\} , \qquad (2\text{-}6)$$

$$E_{\phi}^{s} = \frac{-ik^3 p \sin\phi}{4\pi\epsilon\rho\rho_b} \sum_{n=1}^{\infty} \frac{2n+1}{n(n+1)} \left\{ \frac{\partial P_n^1(\cos\theta)}{\partial\theta} \zeta_n(\rho_b)\zeta_n(\rho)\, a_n(\rho_a) \right.$$

$$\left. + \frac{P_n^1(\cos\theta)}{\sin\theta} \zeta_n'(\rho_b)\zeta_n'(\rho)\, b_n(\rho_a) \right\},$$

where

$$\rho_b = kb$$

In the above it is assumed that $\rho_b > \rho$; for $\rho_b < \rho$, ρ and ρ_b are interchanged.

The solution for an arbitrarily oriented dipole is the superposition of the results for a horizontal dipole and one directed radially, a so-called vertical dipole. The latter solution was obtained in 1918 by Watson (Ref.69). It can be given in the following form for $\rho < \rho_b$ and dipole moment $p\hat{z}$:

$$E_r = -\frac{ik^3 p}{4\pi\epsilon\rho^2\rho_b^2} \sum_{n=0}^{\infty} (2n+1)\, n(n+1)\, P_n(\cos\theta) \frac{\zeta_n(\rho_b)}{\zeta_n'(\rho_a)} \left[\psi_n'(\rho_a)\, \zeta_n(\rho) \right. \tag{2-7}$$

$$\left. - \psi_n(\rho)\, \zeta_n'(\rho_a) \right],$$

$$E_\theta = -\frac{ik^3 p}{4\pi\epsilon\rho\rho_b^2} \sum_{n=0}^{\infty} (2n+1)\, P_n^1(\cos\theta) \frac{\zeta_n(\rho_b)}{\zeta_n'(\rho_a)} \times \left[\psi_n'(\rho_a)\zeta_n'(\rho) - \psi_n'(\rho)\,\zeta_n'(\rho_a)\right] \tag{2-7}$$

$$E_\phi = 0$$

2.4 ALTERNATE FORMS

The early terms in the previous series are oscillatory and as previously pointed out it is necessary to use more than ρ_a terms in evaluating the sum. This slow convergence for large ρ_a and the fairly complicated forms of the individual terms have prompted many attempts to replace these series by forms more suitable for computation and to understand the physical situation. Results of two alternative methods are summarized below.

2.4.1 WATSON TRANSFORMS

Most attempts along the above lines use variations of a contour integration method by Watson (Ref. 69) to convert series (2-7) to a much more rapidly converging series of terms involving functions of complex order. Results of this type for the horizontal dipole case are given here. To illustrate the general procedure, the detailed derivation is given in Section V. This example is chosen since the derivation does not appear explicitly in the literature. The results are, however,

implicitly contained in Felsen (Ref. 17) who derives these rapidly converging series by direct methods. Also, a neat asymptotic form for the backscattering radar cross-section obtained by Scott, (Ref. 51), using a variation of Watson's method, is presented.

The functions which appear in the results below are not tabulated. One must resort to asymptotic forms for their evaluation. As a result they are not preferable to the Mie type series for computational purposes unless ρ_a is very large, as in problems of diffraction of radio waves along the earth. They are of interest, however, in aiding the physical insight into the problem as will be discussed in Section 2.6.

2.4.1 (a) Total Field, Horizontal Dipole

For a horizontal dipole, the expression for the total field is

$$E_\theta = \frac{-ik^3 p \cos\phi}{4\epsilon\rho\rho_b} \sum_{\ell=1}^{\infty} \left\{ \frac{(2n_\ell+1)}{n_\ell(n_\ell+1)\sin(n_\ell\pi)} \frac{P_n^1(-\cos\theta)}{\sin\theta} \frac{\zeta_{n_\ell}(\rho_b)\psi_{n_\ell}(\rho_a)\zeta_{n_\ell}(\rho)}{\left[\frac{\partial \zeta_n(\rho_a)}{\partial n}\right]_{n=n_\ell}} \right.$$

(2-8)

$$\left. + \frac{(2s_\ell+1)}{s_\ell(s_\ell+1)\sin(s_\ell\pi)} \frac{\partial P_s^1(-\cos\theta)}{\partial\theta} \frac{\zeta'_{s_\ell}(\rho_b)\psi'_{s_\ell}(\rho_a)\zeta'_{s_\ell}(\rho)}{\left[\frac{\partial \zeta'_s(\rho_a)}{\partial s}\right]_{s=s_\ell}} \right\}$$

where $\zeta_{n_\ell}(\rho_a) = 0$ and $\zeta'_{s_\ell}(\rho_a) = 0$.

$$E_\phi = \frac{ik^3 p \sin\phi}{4\epsilon\rho\rho_b} \sum_{\ell=1}^{\infty} \left\{ \frac{2n_\ell + 1}{n_\ell(n_\ell+1)\sin(n_\ell\pi)} \frac{\partial P_{n_\ell}^1(-\cos\theta)}{\partial\theta} \frac{\zeta_{n_\ell}(\rho_b)\,\psi_{n_\ell}(\rho_a)\,\zeta_{n_\ell}(\rho)}{\left[\frac{\partial}{\partial n}\left[\zeta_n(\rho_a)\right]\right]_{n=s_\ell}} \right.$$

$$\left. + \frac{2s_\ell + 1}{s_\ell(s_\ell+1)} \frac{P_{s_\ell}^1(-\cos\theta)}{\sin(s_\ell\pi)} \frac{\zeta'_{s_\ell}(\rho_a)\,\psi'_{s_\ell}(\rho_a)\,\zeta'_{s_\ell}(\rho)}{\left[\frac{\partial}{\partial s}\left[\zeta'_s(\rho_a)\right]\right]_{s=n_\ell}} \right\}$$

For large ρ_a Franz (Ref. 20) gives the following

$$n_\ell = \rho_a + \left(\frac{\rho_a}{6}\right)^{1/3} \cdot e^{i\pi/3} \cdot \bar{q}_\ell - \left(\frac{6}{\rho_a}\right)^{1/3} \cdot e^{-i\pi/3} \cdot \frac{\bar{q}_\ell^2}{180} \quad ,$$

$$s_\ell = \rho_a + \left(\frac{\rho_a}{6}\right)^{1/3} \cdot e^{i\pi/3}\, q_\ell + \left(\frac{6}{\rho_a}\right)^{1/3} e^{-i\pi/3} \left(\frac{3}{20 q_\ell} - \frac{q_\ell^2}{180}\right)$$

and

ℓ	q_ℓ	$\bar{q}_\ell$
1	1.469354	3.372134
2	4.684712	5.895843
3	6.951786	7.962025
4	8.889027	9.788127
5	10.632519	11.457423

It is shown in Section 5.3 that there is rapid convergence only in a region which lies entirely in the geometric shadow. An expression useful in the irradiated region may be obtained from (2-8) as shown in Section 5.4 . The result for E_θ is:

$$E_\theta = -\frac{ik^3 p\cos\phi}{4\epsilon\rho\rho_b}\sum_{\ell=1}^{\infty}\left\{\frac{(2n_\ell+1)e^{in_\ell\pi}}{n_\ell(n_\ell+1)\sin(n_\ell\pi)}\frac{P^1_{n_\ell}(\cos\theta)}{\sin\theta}\frac{\zeta_{n_\ell}(\rho_b)\psi_{n_\ell}(\rho_a)\zeta_{n_\ell}(\rho)}{\left[\partial\zeta_n(\rho_a)/\partial n\right]_{n=n_\ell}}\right.$$

$$\left.+\frac{(2s_\ell+1)e^{is_\ell\pi}}{s_\ell(s_\ell+1)\sin(s_\ell\pi)}\frac{\partial P^1_{s_\ell}(\cos\theta)}{\partial\theta}\frac{\zeta'_{s_\ell}(\rho_b)\psi'_{s_\ell}(\rho_a)\zeta'_{s_\ell}(\rho)}{\left[\partial\zeta'_n(\rho_a)/\partial n\right]_{n=s_\ell}}\right\} \qquad (2\text{-}9)$$

$$+\frac{2}{\pi\sin\theta}\int_C\frac{\mu G_{\mu-\frac{1}{2}}}{\mu^2-\frac{1}{4}}\frac{\zeta_{\mu-\frac{1}{2}}(\rho_b)}{\zeta_{\mu-\frac{1}{2}}(\rho_a)}\left[\zeta_{\mu-\frac{1}{2}}(\rho)\,\psi_{\mu-\frac{1}{2}}(\rho_a)-\zeta_{\mu-\frac{1}{2}}(\rho_a)\,\psi_{\mu-\frac{1}{2}}(\rho)\right]d\mu$$

$$+\frac{2}{\pi}\int_C\frac{\mu G'_{\mu-\frac{1}{2}}}{\mu^2-\frac{1}{4}}\frac{\zeta'_{\mu-\frac{1}{2}}(\rho_b)}{\zeta'_{\mu-\frac{1}{2}}(\rho_a)}\left[\zeta'_{\mu-\frac{1}{2}}(\rho)\psi'_{\mu-\frac{1}{2}}(\rho_a)-\zeta'_{\mu-\frac{1}{2}}(\rho_a)\,\psi'_{\mu-\frac{1}{2}}(\rho)\right]d\mu,$$

where

$$G_\mu = \tfrac{1}{2}P^1_\mu(\cos\theta)+\frac{1}{i\pi}Q^1_\mu(\cos\theta),$$

and the contour C is shown in Figure 2.

FIG. 2 THE CONTOUR C

The series here converges rapidly and the integrals can be approximated by a saddle point evaluation. In Section V the first term of such an evaluation is shown to be the geometric optics total field.

The individual terms in the series presented in this section have been given physical interpretations. The validity of these interpretations is a controversial topic and is one of the chief topics discussed in Section 2.6.

2.4.1 (b) Backscattered Field; Incident Plane Wave

An asymptotic series for the backscattering cross-section of a conducting sphere has been obtained by J. M. C. Scott (Ref. 51). It is intended to be useful for spheres for which $a > 2\lambda$. Scott uses the series (2-3) evaluated for $\theta = 0$ and instead of employing the contour used by Watson for his transformation method (See Section V) Scott uses a contour which passes over a saddle point near the origin. In the course of the investigation the approximate expressions for Bessel functions of large, nearly equal, order and argument are extended to higher order terms than those given by Watson and Nicholson.

Scott's result is for

$$S(\rho_a) = \frac{2\pi i}{\lambda} \left. \frac{E_\theta^s}{\cos\phi\, e^{i(\omega t - \rho)}} \right|_{\theta = 0}$$

$$= \frac{2\pi i}{\lambda} \left. \frac{E_\phi^s}{\sin\phi\, e^{i(\omega t - \rho)}} \right|_{\theta = 0} .$$

He obtains

$$S(\rho_a) = -\tfrac{1}{2} i\, e^{2i\rho_a} \left\{ \rho_a + \frac{i}{2} + 2.71517\, \rho_a^{4/3} \exp \left[-2.20000\, \rho_a^{1/3} \right. \right. \qquad (2\text{-}10)$$

$$\left. \left. - i(2+\pi)\, \rho_a - i(0.404308\pi \rho_a^{1/3}) + 2i\pi/3 \right] \right\} .$$

2.4.2 Series in Legendre Polynomials

There are computational advantages to expressing the series (2-3) (or derived functions such as cross-sections or Stokes parameters) as

series of Legendre Polynomials $P_n(\cos\theta)$. The P_n are more extensively tabulated than the P_n^1 or $\frac{dP_n^1}{d\theta}$ functions, interpolation is simpler and there is only one angular function involved. The expansions in the P_n form also aid greatly in handling scattering by clouds of scatterers of mixed sizes.

For these reasons Sekera (Ref. 52) has expressed the series (2-3) and the related bistatic cross-sections for matched as well as crossed polarizations (the elements in the general scattering matrix) as series of the form

$$\sum_{k=o}^{\infty} C_k(\rho_a, \eta)\, P_k(\cos\theta)$$

and computed short tables of the coefficients.

Independently, Chu and Churchill (Ref. 13) have obtained the series for the bistatic radar cross-section and have programmed the result for computations on the Michigan Digital Automatic-Computer (MIDAC). Some computations have been completed but are not published as yet.

2.5 PHYSICAL OPTICS APPROXIMATION

For the scattering of a plane wave by a perfectly conducting body, the physical optics scattered field is given by

$$\vec{H}_{sc} = \frac{1}{4\pi} \int_S (\hat{n} \times \vec{H}) \times \nabla \left(\frac{e^{ikR}}{R} \right) ds \qquad (2\text{-}11)$$

where

$\hat{n}$ = the unit outward normal to the surface S, of the scattering body,

R = the distance between the receiver and the integration point,

$k = 2\pi/\lambda$ (λ = wavelength),

$$\vec{H} = \begin{cases} 2\hat{a}H_o e^{ik(\hat{k} \cdot \vec{r})} & \text{on the geometrically illuminated part of S} \\ 0 & \text{on the geometrically shadowed part of S,} \end{cases}$$

H_o = amplitude of the incident magnetic field,

$\hat{a}$ = unit vector in the direction of the incident magnetic field,

$\hat{k}$ = unit vector in the propagation direction of the incident radiation,

$\vec{r}$ = the vector from the origin to the integration point.

For a sphere of radius a, and $R >> a$, this yields

$$\frac{\sigma(\theta)}{\pi a^2} \cong (2ka)^2 \left| \int_0^{\pi/2} \sin\beta \cos\beta \, J_o(ka \sin\theta \sin\beta) e^{ika(1+\cos\theta)\cos\beta} \, d\beta \right|^2 \qquad (2\text{-}12)$$

where $\sigma(\theta)$ is the radar cross-section, θ the angle between $\hat{k}$ and the radius vector to the receiver ($\theta = 0$ is backscattering), and $J_o(x)$ is

the zero order Bessel function. σ has been computed as a function of θ for ka = 5 and 100 (Fig. 6) and as a function of ka for backscattering (Figure 5). For backscattering, the integral gives

$$\frac{\sigma(0)}{\pi a^2} = 1 - \frac{\sin 2\rho_a}{\rho_a} + \frac{1 - \cos 2\rho_a}{2\rho_a^2} \qquad (2\text{-}13)$$

It is seen that the physical optics result is a good approximation for large enough ka since it is then nearly the geometric optics field (as is the exact solution). However, the manner in which the physical optics result approaches geometric optics is in serious disagreement with that of the exact solution (the amplitude of the physical optics oscillations about geometric optics gives some idea about the amplitude of the true oscillations for values of ka as large as shown, but a random choice in phase and period of these oscillations is just as accurate a guess as physical optics). This is due to the fact that the physical optics correction terms come from the assumed discontinuity in the field at the shadow boundary. That this is a poor assumption may be seen from Fock's expression (Ref. 19)* for the width d, of the penumbra region,

---

* The $\lambda^{1/3}$ dependence of the width of the penumbra region is also obtained in Reference 22. Detailed treatments of the field in this transition region are given by Bremmer (Ref. 10) and Fock (Ref. 18) using integral forms for the field.

$d = (\lambda_a[2/\pi])^{1/3}$, showing that as λ decreases the field becomes more slowly varying with respect to the wavelength. See Section 3.1.1 for further discussion.

2.6 ON PHYSICAL INTERPRETATIONS OF THE FORMULAS

The terms in the different expansions for the fields may be interpreted in various ways. However, not all the interpretations are considered valid by the various workers in electromagnetic theory. In this section we shall discuss briefly the various interpretations and indicate where much more complete treatments will be found. However, we shall go into detail attempting to clarify some of the controversial points.

First of all, each term in the Mie series (2-3) has the form of the field due to a multipole source located at the origin. This is discussed in Stratton (Ref. 60).

Next we consider the series in Section 2.3. By studying the individual terms for small wavelength, i.e., in the approach to geometric optics, Bremmer (Ref. 10*), for example, shows how each term is composed

---

* The material in Reference 10 to which we refer here and elsewhere in this report, appeared originally in a series of papers by van der Pol and Bremmer in the London Philosophical Magazine during 1937 - 1939.

of two systems of waves whose directions of travel are in the same direction radially but in opposite senses in the θ-direction. The amplitudes of each are the same, so the result is a system of waves standing in the θ-direction and traveling in the r-direction.

In like manner Bremmer shows that the terms in the Watson type series for a perfect conductor represent travelling waves in the θ-direction and standing waves in the r-direction for large r. Various authors term these waves "residue waves", "creeping waves" or "radial modes". The validity of some aspects of this interpretation is the controversial point mentioned above and will shortly be discussed in more detail.

Before going on, however, we point out that there are additional terms which occur when the sphere is a non-perfect conductor. These are arranged by Bremmer so they can be interpreted as waves which are refracted into the sphere and undergo various reflections before emerging. The refracted waves are dominant for scattering by water drops (Ref. 66), negligible for problems in which the antenna is near the earth (Ref. 10). These terms may be more or less important than the creeping wave terms, depending on the complex dielectric constant of the sphere material and the sphere size in wavelengths. Bremmer's interpretations are modified in some respects by Ljunggren (Ref. 39) as the result of his independent analysis. Fock (Ref. 18) and Franz and Beckmann (Ref. 21) also give interpretations of this type, the latter being in disagreement with some

aspects of Bremmer's work.

The physics of the situation and its use by various authors to develop approximate solutions to the fields are extensively discussed by van de Hulst (Refs. 65 and 66).

Returning now to the problem of the "creeping wave", the terms in the residue series are interpreted in Franz' work as due to waves which have travelled a number of times around the sphere, attenuating and leaking energy tangentially all the while.* The series being given this interpretation is written for a steady state sinusoidal field, yet the idea of counting the number of times a wave has encircled the sphere implies a non-stationary process. That is, a physically reasonable approach to the identification in the steady state solution of a wave which has travelled around the body a certain number of times is to look at the problem of a sinusoidal incident field (frequency ω) which is turned on at time $t = 0$, and to follow the wave front as it passes around the body.

This approach is essentially contained in Friedlander's paper (Ref. 22) in which scattering from a cylinder is treated. Although (as pointed out by Wu in Reference 71) there is some difficulty in obtaining a solution for the sphere which is analogous in form to Friedlander's solution, we

---

* Franz' argument leading to this interpretation appears to be in error. This is discussed later in this section.

shall nevertheless discuss the latter in some detail because of the considerable similarity between the two problems. The Green's function (the field due to a pulsed source at $(r,\theta,t) = (r_0,0,0)$)is obtained for the cylinder in the form

$$G(r,\theta,t;r_0) = \sum_{m=-\infty}^{\infty} F(r,\theta + 2m\pi,t;r_0) \qquad (2\text{-}14)$$

in which

$$F(r,\theta,t;r_0)=\frac{-1}{4i}\int_{-\infty}^{\infty} d\nu \int_{-\infty}^{\infty} d\omega \left[J_\nu (\omega r) H_\nu^{(1)}(\omega r_0) - \frac{J_\nu'(\omega) H_\nu^{(1)}(\omega r_0)}{H_\nu^{(2)}(\omega)} H_\nu^{(1)}(\omega r) \right] e^{i(\nu\theta-\omega t)}, \qquad (2\text{-}15)$$

where $r< r_0, -\infty < \theta < \infty$

and for $r > r_0$, r and r_0 are interchanged. (The boundary condition is the vanishing of the normal derivative at the surface. The units are chosen so that the radius of the sphere and the velocity of light are equal to unity). $F(r,\theta,t;r_0)$ is the solution of

$$\frac{\partial^2 F}{\partial t^2} - \nabla^2 F = \frac{2\pi}{r_0} \delta(r-r_0)\, \delta(\theta)\, \delta(t), \qquad (2\text{-}16)$$

for $\quad -\infty < \theta < \infty$

with

$$\left.\frac{\partial F}{\partial r}\right|_{r=1} = 0$$

and the radiation condition.

An important property* of the solution of Equation (2-16) is

$$F(r,\theta + 2m\pi,t;r_o) = 0 \text{ for } t \leq \tau_m \qquad (2\text{-}17)$$

where

$$\tau_m = \delta_m + \sqrt{r^2-1} + \sqrt{r_o^2-1} \qquad (2\text{-}18)$$

in which

$$\delta_m = \begin{cases} 2m\pi + \theta - \cos^{-1}\left(\frac{1}{r}\right) - \cos^{-1}\left(\frac{1}{r_o}\right) & m \geq 0 \\ -2m\pi - \theta - \cos^{-1}\left(\frac{1}{r}\right) - \cos^{-1}\left(\frac{1}{r_o}\right) & m < 0 \end{cases} \qquad (2\text{-}19)$$

* Friedlander gives this seemingly reasonable property, stating, without proof, that it is true because a previous result (Ref. 23) of his on the extension of Fermat's theorem to diffracted wavefronts, can be extended to propagation in the Riemann surface, $0 \leq r < \infty$, $-\infty < \theta < \infty$, the sheets of which are given by $(2m-1)\pi \leq \theta \leq (2m+1)\pi$, $m = 0, \pm 1, \ldots$.

The physical interpretation of these results is given in detail in Reference 22. We discuss this briefly. Consider $0 \leq \theta \leq \pi$. At a point (r,θ) in the geometric shadow region, the field is zero for $t \leq \tau_0$, the time for a light ray to travel the shortest path between $(r_0,0)$ and (r,θ) (see Figure 3).

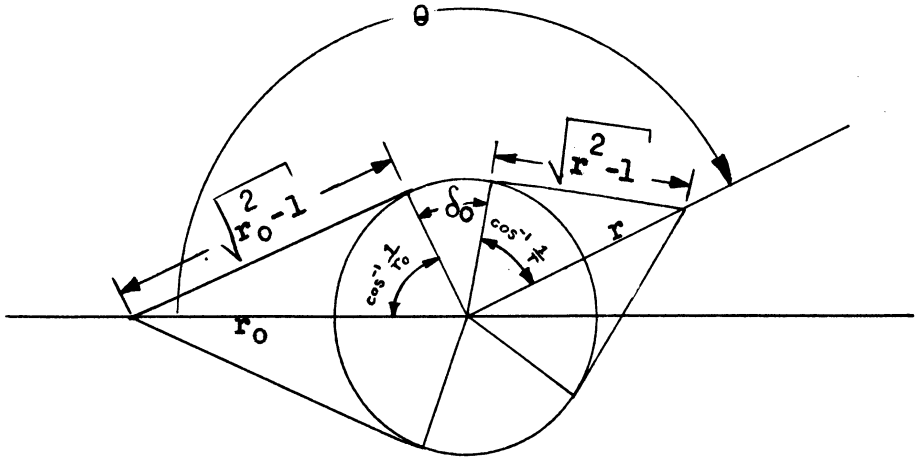

FIG. 3 GEOMETRY OF THE CYLINDER DISCUSSION

At τ_0 the diffracted front D', (see Reference 23 for the extension of Fermat's principle to diffraction) traveling clockwise arrives, and until τ_{-1}, the time of the arrival of the diffracted front D", traveling counterclockwise, the field is

$$G(r,\theta,t;r_0)=F(r,\theta,t;r_0), \qquad \tau_0 \leq t \leq \tau_{-1} \quad . \qquad (2\text{-}20)$$

For $\tau_{-1} \le t \le \tau_1$ ($\tau_1 - \tau_0 = 2\pi$ is the time for a diffracted front to pass once around the cylinder), we have

$$G(r,\theta,t;r_0)=F(r,\theta,t;r_0)+F(r,\theta-2\pi,t;r_0). \tag{2-21}$$

Continuing,

$$G(r,\theta,t;r_0)=F(r,\theta,t;r_0)+F(r,\theta-2\pi,t;r_0)+F(r,\theta+2\pi,t;r_0), \tau_1 \le t \le \tau_2; \tag{2-22}$$

etc.

A similar type of result is obtained for any source time-function,

$$S(t)= 1(t)\, s(t),$$

which is "turned on" at time t = 0; here $1(t)$ is the step-function

$$1(t)= \begin{cases} 1, & t \ge 0 \\ 0, & t < 0 \end{cases} . \tag{2-23}$$

For then the solution, $\mathcal{H}$, which satisfies

$$\frac{\partial^2 \mathcal{H}}{\partial t^2} - \nabla^2 \mathcal{H} = 2\pi\, \delta(x-r_0)\, \delta(y)\, s(t)\, 1(t),$$

is given by

$$\mathcal{H} = \int_0^\infty dt'\, G(r,\theta,t-t';r_0)\, s(t') = \int_{-\infty}^{t} dt'\, G(r,\theta,t';r_0)\, s(t-t'). \tag{2-24}$$

Writing

$$F(r,\theta+2n\pi,t;r_o)= G_n(t), \tag{2-25}$$

we have

$$\mathcal{H} = \sum_{n=-\infty}^{\infty} \mathcal{H}_n(t), \tag{2-26}$$

where

$$\mathcal{H}_n(t)= 1(t-\tau_n) \int_{\tau_n}^{t} dt'\, G_n(t')\, s(t-t') \quad . \tag{2-27}$$

In particular, for

$$s(t) = e^{-i\omega t},$$

$$\begin{aligned} \mathcal{H}_n(\omega,t) &= 1(t-\tau_n)e^{-i\omega t} \int_{\tau_n}^{t} dt'\, G_n(t')e^{i\omega t'} \\ &= 1(t-\tau_n)e^{-i\omega t} \int_{-\infty}^{t} dt'\, G_n(t')e^{i\omega t'} \quad . \end{aligned} \tag{2-28}$$

In terms of the above interpretation, each function $\mathcal{H}_n(\omega,t)$ can properly be termed the wave which has passed around the cylinder n times, or, more precisely the field corresponding to the n'th passage of the wave front around the body. In the limit $t \longrightarrow \infty$, $\mathcal{H}_n(\omega,t) \longrightarrow$ the

Fourier transform of $G_n(t)$. To compare this definition with that of Franz, we first write, following Friedlander, the Fourier transform ($e^{-i\omega t}$ times which is the solution of the steady state problem),

$$\mathcal{F}(r,\theta,\omega;r_o)=\frac{1}{4i}\int_{-\infty}^{\infty} d\nu\, H_\nu^{(1)}(\omega r_o)\left[J_\nu(\omega r)-\frac{J_\nu'(\omega)H_\nu^{(1)}(\omega r)}{H_\nu^{(1)'}(\omega)}\right]e^{i\nu\theta} \quad (2\text{-}29)$$

as a sum of residues of the integrand at the zeros, ν_ℓ, of $H_\nu^{(1)'}(\omega)$ in the upper half ν-plane:

$$\mathcal{F}(r,\theta,\omega;r_o)=\frac{\pi}{2}\sum_{\ell=1}^{\infty}\frac{J_{\nu_\ell}'(\omega)H_{\nu_\ell}^{(1)}(\omega r_o)H_{\nu_\ell}^{(1)}(\omega r)}{\left[\frac{\partial H_\nu^{(1)'}(\omega)}{\partial\nu}\right]_{\nu=\nu_\ell}}e^{i\nu_\ell|\theta|} \quad (2\text{-}30)$$

valid for both $r>r_o$ and $r\leq r_o$. For $0\leq\theta\leq\pi$, the field corresponding to the n'th passage of the wave front may be written

$$\mathcal{F}(r,\theta+2n\pi,\omega;r_o)=\frac{\pi}{2}\sum_{\ell=1}^{\infty}K_\ell\begin{cases}e^{i\nu_\ell(\theta+2n\pi)} & n\geq 0\\ e^{-i\nu_\ell(\theta+2n\pi)} & n<0\end{cases} \quad (2\text{-}31)$$

where

$$K_\ell = \frac{J'_{\nu_\ell}(\omega) H^{(1)}_{\nu_\ell}(\omega r_o) H^{(1)}_{\nu_\ell}(\omega r)}{\left[\frac{\partial H^{(1)'}_\nu(\omega)}{\partial \nu}\right]_{\nu=\nu_\ell}}$$

Franz' corresponding result is

$$G_{Fr} = \frac{i\pi}{2} \sum_{\ell=1}^{\infty} \frac{\cos \nu_\ell (\theta - \pi)}{\sin \nu_\ell \pi} K_\ell$$

$$= \frac{\pi}{2} \sum_{\ell=1}^{\infty} \frac{e^{i\nu_\ell \theta} + e^{i\nu_\ell (2\pi - \theta)}}{1 - e^{2i\nu_\ell \pi}} K_\ell$$

$$G_{Fr} = \frac{\pi}{2} \sum_{n=0}^{\infty} \sum_{\ell=1}^{\infty} K_\ell \left[e^{i\nu_\ell (\theta + 2n\pi)} + e^{i\nu_\ell (2\pi - \theta + 2n\pi)} \right] \quad (2\text{-}32)$$

Thus it is apparent that Franz' statement that the denominator $1-e^{2i\nu_\ell \pi}$ corresponds to the sum of creeping waves which have encircled the cylinder

one, two and more times is in accord with the concepts of Friedlander.*

Both Friedlander and Franz give a physical interpretation to the individual terms (different ℓ) of Equation (2-31) (the former using the term "propagation modes", the latter calling each term a "creeping wave"). For large ω (large ratio of radius to wavelength), Friedlander obtains approximate expressions for the terms

$$\mathcal{F}_{n,\ell} = \frac{\pi}{2} K_\ell \begin{cases} e^{i\nu_\ell (\theta+2n\pi)} & n \geq 0 \\ e^{-i\nu_\ell (\theta+2n\pi)} & n < 0 \end{cases} \qquad (2\text{-}33)$$

in the case $r_o \to \infty$ (incident plane wave) and $r = 1$ (observation point on the cylinder surface), each one of which terms he interprets as a simple wave with phase velocity $d\theta/dt = (1+\frac{1}{2}\alpha_\ell \omega^{-2/3})^{-1}$, and subject to an exponential attentuation which reduces the amplitude by 1/e in the

---

* Wu (Ref. 71) has carefully defined creeping waves in terms of the solution (for two-dimensional bodies) on the infinite-sheeted Riemann surface in apparently the same way as Friedlander (Wu doing this for cylinders of arbitrary shape). Hence the above statement of Franz is apparently in accord with Wu's work as well. However Wu states that his asymptotic formula for the creeping wave is essentially different from that of Franz. (Our discussion of Wu's work is based mainly on conversation with Drs. Wu, Rubinow, and Kodis of Harvard since Ref. 71 was not received until this report was being prepared for reproduction.)

distance $3^{-\frac{1}{2}}\alpha_\ell^{-1}\omega^{-1/3}$. (The α_ℓ are the zeros of the Airy function $\mathrm{Ai}(-2^{1/3}\alpha)$).

The erroneous argument of Franz referred to previously is the following. For large ω, Franz obtains the expression (for $e^{-i\omega t}$ time-dependence)

$$G \cong -\frac{\pi}{4} e^{-i\pi/6}\left(\frac{\omega}{6}\right)^{1/3} f(r_0)f(r)\sum_\ell \frac{e^{i\nu_\ell\theta} + e^{i\nu_\ell(2\pi-\theta)}}{1-e^{2\pi i\nu_\ell}} \frac{e^{-i\nu_\ell(\cos^{-1}\frac{1}{r}+\cos^{-1}\frac{1}{r_0})}}{q_\ell\,\mathrm{Ai}^2(q_\ell)} \qquad (2\text{-}34)$$

where

$$f(r) = \frac{e^{i\left[\omega\sqrt{r^2-1}-\pi/4\right]}}{\sqrt{\omega\sqrt{r^2-1}}}\ ; \qquad (2\text{-}35)$$

(This is Equation (25) in Reference 20; $q_\ell \mathrm{Ai}^2(q_\ell)$ is a function of ν_ℓ, the exact form of which is irrelevant here. We have put a=1; c=1; $\rho_1, \rho_2 = r_0, r$; $\phi = \theta$.) It is stated that this is a good approximation when $\omega(r-1)$ and $\omega(r_0-1)$ are at least of the order of $\omega^{1/3}$, i.e.,

$$\begin{aligned}(r-1)\omega &\gtrsim \omega^{1/3}\\ (r_0-1)\omega &\gtrsim \omega^{1/3}\end{aligned} \qquad (2\text{-}36)$$

Translating from Franz' article:

"One recognizes as a factor in these expressions the cylindrical wave running from P_1 to P_2 to the edge of the visible (or illuminated) surface region, and furthermore (under the summation) phase terms with damping (corresponding to the imaginary part of ν) which correspond to angular displacements of

$$\Theta - \cos^{-1}\frac{1}{r} - \cos^{-1}\frac{1}{r_o}$$

and

$$2\pi - \Theta - \cos^{-1}\frac{1}{r} - \cos^{-1}\frac{1}{r_o} \quad ."$$

The factor referred to is clearly $f(r)$ or $f(r_o)$. We point out that neither $f(r)$ nor $f(r_o)$ are cylindrical waves "running from P_1 to P_2". This is obvious since $f(r)$ comes as an approximation to the Hankel function (which is independent of Θ) and the Poynting vector for any solution of the wave equation which is independent of Θ (and $\emptyset$) must be in the radial direction. That is, the Poynting vector associated with the factor $f(r)$ is along radii of the cylinder and not tangent to the cylinder. We have checked the interpretation of the individual modes by computing the Poynting vector, $\vec{S}$, for a single propagation mode in the approximation of Equation (2-33). It turns out that $\vec{S}$ is in agreement with Franz' result, namely it is approximately parallel to the line

tangent to the cylinder and passing through the observation point provided

$$(r - 1)\omega \gg \omega^{1/3},\ (r_o - 1)\omega \gg \omega^{1/3} \quad . \qquad (2\text{-}37)$$

Incidentally, we feel that Franz' condition (2-36) above is not strong enough and should be replaced by the inequality (2-37).

2.7 CONCENTRIC SPHERES

Considerable practical importance is attached to solutions for the scattering of electromagnetic waves by coated spheres, i.e. spheres covered with a layer of uniform thickness of a second material. This problem includes, as a special case, spherical shells. It is of interest to meteorologists in the field of radar observation of weather phenomena since, for example, an ice sphere covered by water roughly represents a melting hailstone. Observation of weather balloons is also of importance. Also, if the inner sphere is metal the solution can be conveniently used in conjunction with experimental investigations of the reflection properties of materials used to coat the sphere.

The general solution for an incident plane wave analogous to Mie's solution for a coated sphere is given explicitly in Reference 3 by Aden and Kerker. In their paper the sphere, the coating, and the embedding medium are each permitted to have arbitrary complex dielectric constants. Scharfman (Ref. 49) specialized these results to the case where the inner sphere was perfectly conducting, the coating was a pure dielectric and

the outer medium was free space. He then carried out numerical and experimental investigations in the resonance region to demonstrate and explain the very interesting result that in this region the dielectric coated spheres have greater backscattering cross-sections than perfectly conducting uncoated spheres whose radius is that of the outer edge of the dielectric layer.

R. V. Alred presented the formulas for coated spheres irradiated by a plane wave in Reference 4 and made numerical calculations for an absorbing coating (Section 3.1.2).

For the case of a radial electric dipole source at a finite distance from a coated sphere a solution is given by Wait (Ref. 68) as an integral order expansion similar to those in Section 2.3 and converted by a Watson-type transformation to a more rapidly converging series of the type given in Section 2.4.1.

2.8 TOTAL SCATTERING AND FORWARD SCATTERING

For many applications there is special interest in either the forward scattered energy or the total scattered energy for plane wave scattering. These are related by

$$Q = 2\lambda \ \mathrm{Im}\, f(\pi) \quad .$$

Here Q is the total cross-section, and $f(\pi)$ is the complex forward scattering amplitude, that is, the coefficient of $\frac{e^{ikr}}{r}$ in the far field form of the solution. These quantities may be computed from the Mie

series. However, for large ρ_a much better means are now available; namely, the use of asymptotic expansions in inverse powers of ρ_a.

For example, Wu and Rubinow (Ref. 72) have obtained corrections to the geometric optics total cross-section for short wavelengths in the case of the sphere and circular cylinder. The method is a direct summation of the eigenfunction expansions (the Mie series for the electromagnetic case) for the forward scattering cross-section, after introduction of the appropriate asymptotic forms. Their results for the Neumann and Dirichlet scalar problems and the electromagnetic problems with the sphere are respectively

$$\frac{\sigma_{Total}}{2\pi a^2} = 1 + \frac{A}{(\rho_a)^{2/3}}, \text{ where } A = \begin{cases} -0.8640 & \text{Neumann} \\ 0.99618 & \text{Dirichlet} \\ 0.0661 & * \text{ Electromagnetic.} \end{cases}$$

Wu (Ref. 71) has used a different representation for the total scattering cross-section and obtained more terms in the asymptotic expansions. His results for the electromagnetic case are:

---

* In the reference a summary of results is given in which the coefficient is listed by error as 0.1322.

$$\frac{\sigma_{\text{Total}}}{2\pi a^2} = 1 + 0.06595661\ \rho_a^{-2/3} + 0.7797489\ \rho_a^{-4/3} - 2.8713350\ \rho_a^{-2} - 0.3385447\ \rho_a^{-8/3} + 0.058460\ \rho_a^{-10/3} + \cdots .$$

Note that the geometric optics cross-section is

$$\lim_{\rho_a \to \infty} \sigma_{\text{total}} = 2\pi a^2 ,$$

twice the geometrical cross-section. It is shown in a very interesting paper by Brillouin (Ref. 11) that half of the energy represented by this cross-section is scattered uniformly around the sphere and half is scattered directly forward to cancel the incident field, thus producing the shadow.

III

COMPUTED RESULTS

In this section we have listed many of the more recent computational results. Description of tables will use a standard abbreviated form given by the example: x = 0(10)100; 5s. This indicates that the function of x under consideration is tabulated for x = 0 to 100 at intervals in x of 10, with results good to 5 significant figures; 5d instead of 5s would indicate 5 decimal place accuracy.

3.1 PLANE INCIDENT WAVES

Fields and cross-sections have been computed from the series given in Equation (2-3) (or the Aden-Kerker series for coated spheres) by several groups as summarized below. Most of these results have been in connection with scattering from particles with a low index of refraction. Additional results may be located by use of a summary list of Mie theory computations recently published by Kerker (Ref. 35).

3.1.1 Backscattering Cross-Section

Several authors have made computations of the cross-section σ, for various values of ρ_a in the perfect conductivity case. These are summarized in Figure 4. It is to be noted that there is considerable discrepancy between the different authors' results at the maxima and minima of the curve. In Figure 5 the corresponding curve computed by physical optics (Ref. 54) is given, as is the curve for the acoustic case of scattering by a rigid sphere (Dirichlet problem for the scalar wave equation). The latter curve is taken from Stenzel (Ref. 59).

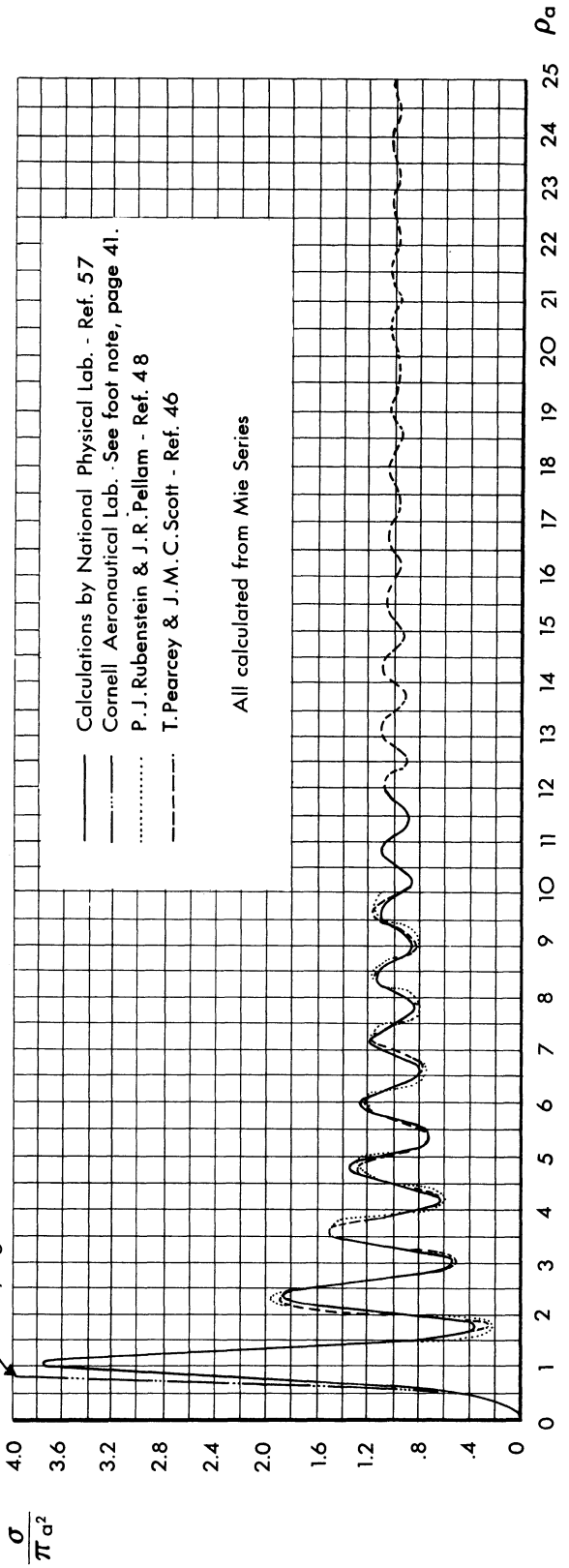

FIG. 4 RADAR CROSS-SECTION, σ, OF A SPHERE, FOR BACKSCATTERING

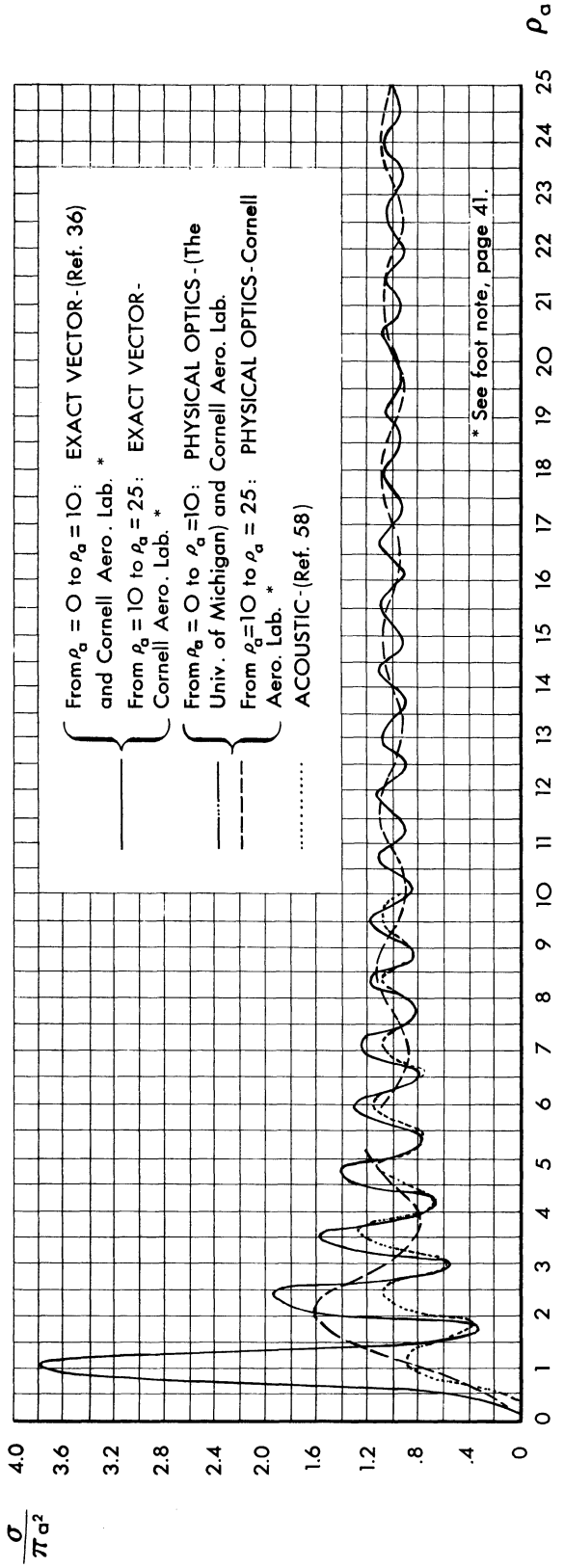

FIG. 5 CROSS-SECTION OF A SPHERE OF RADIUS a FOR BACKSCATTERING; COMPARISION OF THEORIES

In addition to plotting the exact and physical optics cross-sections R. G. Kell and V. E. Pound* have computed the vector difference between the exact and physical optics backscattered fields and plotted $C = \frac{2}{a\lambda}$ times the magnitude of the result vs. ρ_a for $0 \leq \rho_a \leq 25$ and also made polar plots of this field.

The acoustical computation predicts the position of the maxima and minima shown by the exact cross-section better than the physical optics cross-section. However, it behaves differently in that the heights of the first three maxima increase for the acoustic cross-section, while they decrease for both the physical optics and exact cross-sections. The physical significance of these comparisons becomes clearer when the prolate spheroid is studied. Discussion of this matter appears in Reference 56. Further discussion of the physical optics result also appears in Section 2.5.

Chiao-Min Chu (Ref. 12) and Kennaugh and Sloan (Ref. 34) have tabulated the backscattering cross-section for water drops at different wavelengths using values of the complex index of refraction taken from J. A. Saxton's well known measurements. Chu computed for

$$\lambda = 1,3,5,7.5, \text{ and } 10 \text{ mm};$$
$$\rho_a = .05(.05).50(.10)1.50(.25)5.00; \text{ 4s}$$

*Private communication from R. G. Kell of the Cornell Aeronautical Lab., Inc., to K. M. Siegel.

Kennaugh and Sloan's computations are based on the coefficients given in Reference 42 for

λ	ρa	n
2.8 mm	.10(.05)1.00(.1)5	3.41 - 1.94i
4.5 mm	.10(.05)1.00(.1)3.0	4.21 - 2.51i
8 mm	.10(.05)1.00(.1)2.0	5.55 - 2.85i
1.6 cm	.100(.025)1.00(.05)1.30	7.20 - 2.65i
2.8 cm	.100(.025)1.000	8.18 - 1.96i
10 cm	.10(.01).30(.005).430(.01).60	8.90 - 0.69i

Aden (Ref. 1) has computed a similar curve for water spheres at λ = 16.230cm corresponding to ϵ = 81 − i 7.8 and various sphere sizes.

3.1.2 Backscattering Cross-Section for Coated Spheres

Based on the Aden and Kerker theoretical results for concentric spheres (Ref. 3) two sets of computations have been made.

One set is by Langleben and Gunn (Ref.38) who have given curves, for water coated ice spheres, of $\sigma(0)$ vs. q_1, the ratio of water mass to total mass and q_2, the ratio of water film thickness to r (the outer radius), for λ = 0.9, 3, and 10cm, $2\pi a/\lambda$ being constant ($\sim$0.1). They also plot the corresponding curves for $\sigma(0)/\sigma(0)_M$; $\sigma(0)_M$ is the value of $\sigma(0)$ when all the ice is melted. This illustrates the rapid rise in cross-section when the ice begins to melt. Furthermore, they show that curves of $\sigma(0)/\sigma(0)_M$ as a function of q_1 or q_2, holding λ fixed, are essentially independent of a as long as $2\pi a/\lambda \ll 1$.

Secondly, computed and experimental backscattering cross-section tables and curves are presented by Scharfman (Ref. 49) for metallic spheres with a ratio of coating thickness to inner sphere radius of 1/6 and relative dielectric constants of the coating

$$\epsilon = 2.56,\ 4,\ 8,\ 10,\ 15,\ 25,\ 50,\ 70,\ 100,\ 1000 \text{ and } 10000.$$

In Reference 4 Alred made a numerical comparison between the magnitude of the field backscattered from a metal sphere coated with an absorbing material of permeability μ and complex relative dielectric constant

$$\epsilon = \frac{\lambda}{\sqrt{2}}\left(1 - \frac{\lambda}{\sqrt{3}}\right) = 2\mu ,$$

as computed by the exact equation and as computed by simply multiplying the geometric optics answer for a metallic sphere by the reflection factor for reflection at normal incidence from an infinite plane metal sheet coated with the material. The results agree to within 15 percent for $\rho_a > 12$.

3.1.3 Bistatic Scattering

There are very extensive computations (based on the Mie series) of quantities measuring bistatic scattering for low indices of refraction n. They include results by

(a) Air Force Cambridge Research Center, Geophysics Research Directorate.

Rudolph Penndorf and his associates have computed a large amount of data being published as separate parts of Reference 47.

In part 7 of Reference 47 the Mie scattering coefficients i_1 and i_2* are given for

$n = 1.33$, $\rho_a = 0.1(0.1)30$

$\theta = 0^\circ(5^\circ)170^\circ$; $170^\circ(1^\circ)180^\circ$; 4s and better for small θ

In parts 8-11, i_1 and i_2 are given for

$n = 1.40, 1.44, 1.486, 1.5$

$\rho_a = 0.1(0.1)30$

$\theta = 0(10^\circ)170^\circ$; $170^\circ(1^\circ)180^\circ$; 4s and better for small θ

(b) The University of Michigan.

Gumprecht and Sliepcevich (Ref. 28) have computed i_1 and i_2 for

$\theta = 90^\circ$

$n = 1.2, 1.33, 1.4, 1.44, 1.50, 1.60$

$\rho_a = 1(1)5(2)10(5)100(10)200(50)400$; 4s ,

Gumprecht et al, (Ref. 30) give i_1 and i_2 for

$n = 1.33$

$\rho_a = 6, 8, 10(5)40$

$\theta = 0(10)180^\circ$; 4s

Unpublished computational results obtained at the Willow Run Laboratories are shown graphically in Figures 6 and 7.

* i_1 and i_2 are respectively the magnitudes squared of the sums in E_ϕ and E_θ, Equation (2-3).

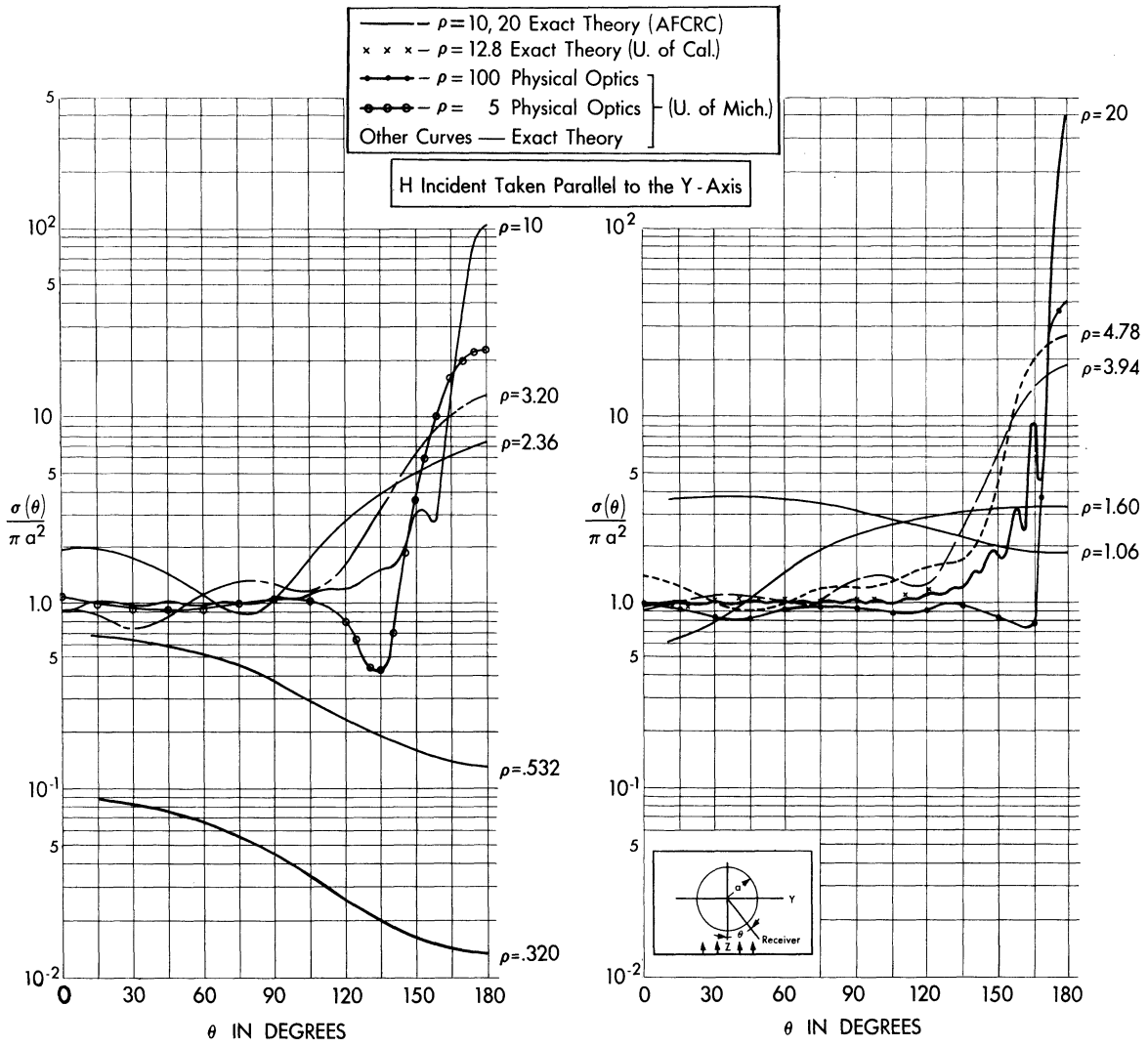

FIG. 6 BISTATIC SPHERE CROSS-SECTIONS — H PLANE

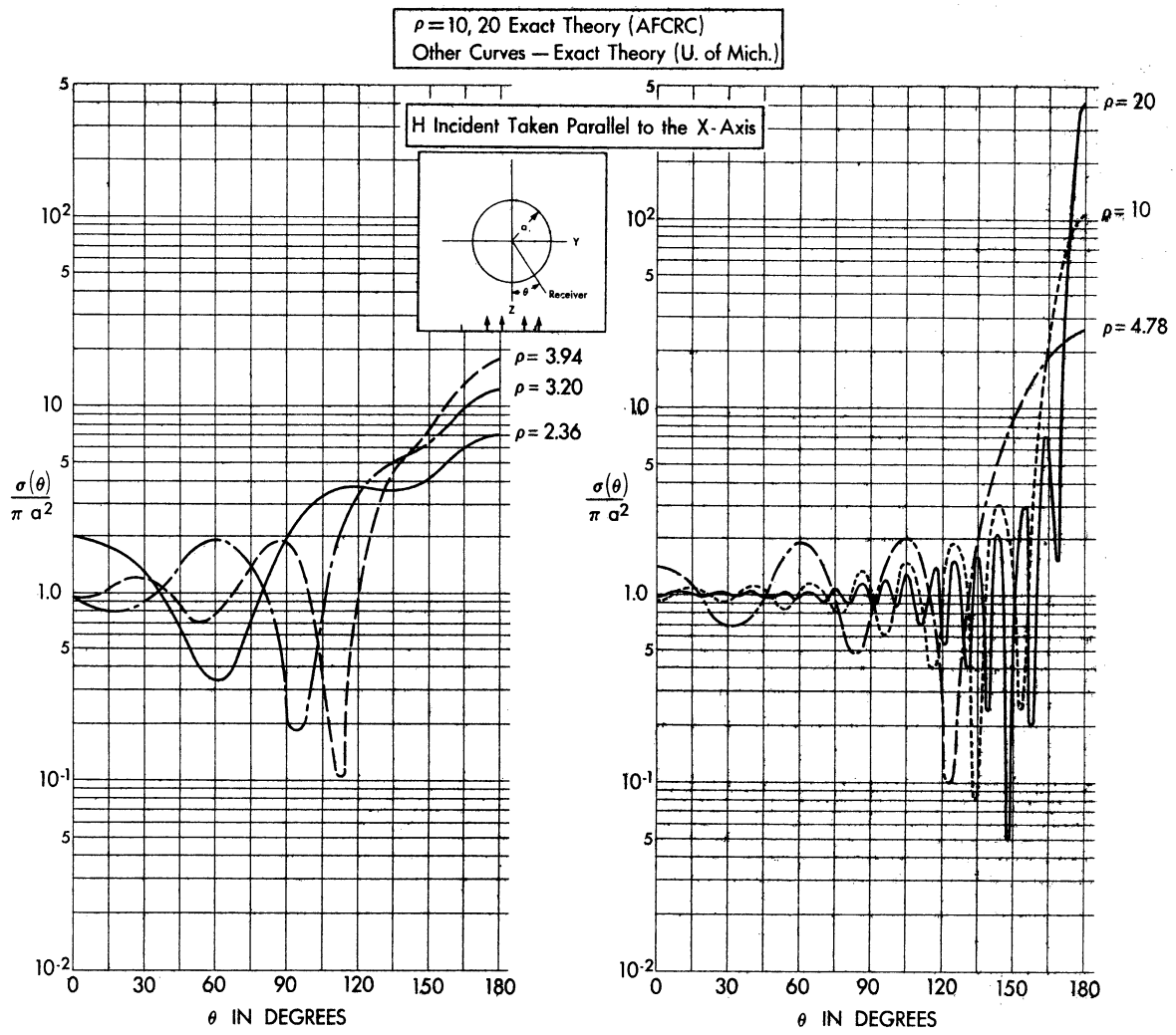

FIG. 7 BISTATIC SPHERE CROSS-SECTIONS — E PLANE

(c) National Bureau of Standards

Tables (computed under the supervision of A. N. Lowan) of i_1 and i_2 (Ref. 42) are available for

$\theta = 0^\circ(10^\circ)180^\circ$; 4s or 6d.

$n = 1.33, 1.44, 1.55, 2.00,$

$\rho_a = .5; .6; 1.0; 1.2; 1.5; 1.8; 2.0; 2.4; 2.5; 3.0; 3.6; 4.0;$
$4.8; 5.0; 6.0.$

For perfectly conducting spheres angular patterns are computed by

(d) University of California at Los Angeles, Dept. of Meteorology.

For the same parameters and accuracy as in (c) O. A. Tweitmoe (Ref. 64) computed the cross-sections corresponding to crossed linear polarizations.

(e) Office of Scientific Research and Development.

V. K. LaMer in Reference 37 gives i_1 and i_2 for

$n = 1.33, 1.44, 1.55, 2.0;$

$\rho_a = 0.5(0.1 \text{ to } 0.5)\ 6.0; \quad \theta = 0(10^\circ)180^\circ$; 4s.

(f) Air Force Cambridge Research Center, Antenna Laboratory.

Under the direction of Nelson Logan the far zone field for

$\rho_a = 1.1(0.6)9, 5, 10, 20; 0 \quad \theta$

are computed and will be published shortly by AFCRC. The pattern is a far more oscillatory function of θ than Blumer's results (Ref. 7) indicate. These curves for $\rho_a = 10$ and 20 are reproduced in Figures 6 and 7. Note that the E plane pattern is much more oscillatory than the H plane pattern which is almost isotropic from 0 to 120 degrees.

(g) University of California, Berkeley.

A scattering curve for $\rho_a = 12.8$ by Hamren (Ref. 31) is shown in Figure 6.

Physical optics as presented in Reference 54 was used at The University of Michigan to compute curves of σ vs. θ for $\rho_a = 5$ and 100. These curves are included in Figure 6.

3.1.4 Total Scattering

The total scattering cross-section Q has been computed by the Mie theory in many places for low indices of refraction. Some of the more extensive tables are those of

(a) The Bureau of Standards (Ref. 42).

n = 1.33, 1.44, 1.55, 2.00 ; ρ_a = 0.5 (variable) 6.0; 3s; (also for the complex indices corresponding to water at various wavelengths as listed in Section 3.1.1 , all to 3d.)

(b) Gumprecht and Sliepcevich (Ref. 28)

n = 1.20, 1.33, 1.40, 1.44, 1.50, 1.60

ρ_a = 1(1)5; 6(2)10, 10(5)100; 100(10)200; 200(50)400; 4s

(c) Chu (Ref. 12)

Computation for total scattering of water spheres are given for the wavelengths and ρ_a values listed in 3.1.1 for backscattering.

3.2 DIPOLE SOURCE ON THE SPHERE

Many computational results are available for the field along the surface of a sphere due to a vertical magnetic or electric dipole, on or near the surface. These are based on the series given in Section 2.4 or on geometric optics, depending on which is more appropriate according to the

magnitude of the straight line distance D between receiver and transmitter.

(a) H. Bremmer.

In Chapter VI of Reference 10 the radial component of the electric field for a vertical electric dipole transmitter and the tangential component for a vertical magnetic dipole are computed. Families of graphs are given of rms electric field E vs. D for average soil (conductivity = 10^{-13} emu, relative dielectric constant = 4) or sea water (conductivity = 4×10^{-11} emu, dielectric constant = 80). The figures cover receiver and transmitter heights h_1 and h_2 both zero,

D = 0 - 2000 km

λ = 60, 100, 150, 200, 300, 450, 600, 1000, 1500, 2000, 5000, 10000, 20000 m.

D = 0 - 200 km

λ = 1, 2, 5, 10, 20, 40, 60, 100, 150, 200, 300, 450, 600, 1000, 2000 m.

D = 0 - 30 km; 0 - 5 km

λ = .03, .10, .20, .40, 1, 2, 5, 10 m.

h_1, h_2 varied

λ = 7 m, soil only; D = 0 - 150 km.

All combinations of

h_1 = 0, 10, 50, 200 m and

h_2 = 0, .93, 1.87, 5, 10, 20, 50, 100, 200 m.

λ = 3m soil only; D = 0 - 150 km

All combinations of

h_1 = 0, 10, 50, 200 m and

h_2 = 0, 5, 10, 20, 50, 100, 200, 500 m.

(b) J. R. Wait.

In Reference 67 the Watson transformation is used to compute the E-plane radiation pattern of a vertical electric dipole at the surface of a large conducting sphere. The computations are compared with the experimental results of Bain (Ref. 6) and of Cohn and Morita (Ref. 14) obtained for slotted spheres which represent the same thing theoretically. The agreement is good for the electrically largest sphere ($\rho_a \cong 550$), but only fair for smaller ρ_a values. The discrepancies are attributed to approximations in the residue series (which are valid only for large ρ_a), and to experimental errors. The computations were made for ρ_a = 550, 131 and 26.2. The angle θ, measured in the E-plane (i.e., perpendicular to the slot) from the slot, ran from 60° to 150°.

3.3 AUXILIARY TABLES FOR EXACT SUMMATION

The functions of ρ and n needed to determine the field directly from the equations (2-3) and (2-6) have been tabulated in various places. The most convenient sources are listed below with details of the tabulation.

3.3.1 The Associated Legendre Function $P_n^1(\cos\theta)$ and Its Derivative $d P_n^1(\cos\theta/d\theta$

An extensive tabulation of these functions is due to Gumprecht and Sliepcevich (Ref. 26) who tabulated them for

$$n = 1(1)420;\ \theta = 0^\circ(10^\circ)170^\circ(1^\circ)180^\circ;\ 5s.$$

N. Logan and G. Reynolds of the Air Force Cambridge Research Center have tabulated P_n^1 and $d P_n^1(\cos\theta)/d\theta$ for

$$n = 1(1)150;\ \theta = 0^\circ(1^\circ)180^\circ;\ 6d.$$

These results will appear in the near future as an AFCRC Electronic Research Directorate report.

Tables (Ref. 43) prepared by the Mathematical Tables Project at the National Bureau of Standards give the above functions for

$$n = 1(1)10;\ \theta = 0(1^\circ)90^\circ;\ 6s.$$

Gucker and Cohn (Ref. 25) tabulate these quantities for

$$n = 1(1)32;\ \theta = 0(2.5)180^\circ;\ 5s.$$

3.3.2 Bessel Functions

In Reference 27 the Ricatti Bessel functions $S_n(x)$ and $C_n(x)$ and their derivatives are tabulated. These functions are related to the functions $\psi_n(x)$ and $\zeta_n(x)$ used in this report by

$$\psi_n(x) = S_n(x) \text{ and } \zeta_n(x) = S_n(x) - i\, C_n(x)\ .$$

Two tables are given. The first lists $S_n(x)$, $S_n'(x)$ and $C_n'(x)$ for

$x = 1(1)6;\ 6(2)10;\ 10(5)100;\ 100(10)200;\ 200(50)400;$ 6d.

The second lists S_n and S_n'

$x = 1.2$ (miscellaneous values)640; 6d.

In all the above, for each value of x, n covers the range from 1 to a number somewhat greater than x, such that n presumably goes high enough to insure that the significant terms in the series may be computed.

Reference 44 prepared by the Mathematical Tables Project gives

$$\sqrt{\frac{\pi}{2x}}\ J_\nu(x) = \frac{1}{x}\,\Psi_{\nu-\frac{1}{2}}(x) \quad .$$

In Vol. I the ranges covered are

$$\pm\nu = \tfrac{1}{2}(1)\ \frac{25}{2}\ ;\ x = 0(.01)\ 10(.1)25;$$

$$\pm\nu = \frac{27}{2}\ ;\ x = 0(.01)\ 10(.05)\ 10.5(.1)25;$$

8s to 10s for $x \leq 10$, mostly to 7s for $x > 10$.

In Vol. II, the ranges covered are

$$\pm\nu = \frac{29}{2}\ (1)\ \frac{43}{2}\ ,\ x = 0(.01)\ 10(.1)25;$$

$$\pm\nu = \frac{45}{2}\ (1)\ \frac{61}{2}\ ,\ x = 10(.1)25$$

8s to 10s for $x \leq 10$, mostly 7s for $x > 10$.

Also given are tables covering the ranges

$\nu = \frac{1}{2}\ (\frac{1}{2})\ \frac{41}{2}, x = 0\ (.1)\ 10,$ 9d; $\nu = \frac{1}{2}\ (1)\ \frac{61}{2}$,

$x = 10(.1)\ 25$; mostly 7s; $-\nu = \frac{29}{2}\ (1)\ \frac{33}{2}$,

$x = 0(.1)\ 9.5(.05)\ 10(.1)\ 25$; mostly 7s,

$-\nu = \frac{35}{2}\ (1)\ \frac{61}{2}$, $x = 0(.1)\ 25$, mostly 9s.

The function ζ_n can be computed from the above data by using the formula

$$\zeta_n(x) = \psi_n(x) - i(-1)^n\ \psi_{-n-1}(x)\ .$$

3.3.3 The Mie Series Coefficients

The coefficients $a_n(\rho_a, \eta)$ and $b_n(\rho_a, \eta)$ are tabulated by themselves in References 12, 28, 43 and 47, for the indices of refraction and ρ_a values given for the scattering functions and for sufficiently large n values to evaluate the series at the θ values for which the scattering functions were tabulated.

IV

EXPERIMENTAL INVESTIGATIONS USING SPHERES

Most of the numerous experimental measurements of scattering from spheres are not absolute measurements but are made for calibration purposes. In the radar field they are made, not to check out Equation (2-3) (which is equivalent to checking Maxwell's electromagnetic equations), but to check the over-all experimental set-up or to obtain the results for other scatterers by measuring their echoes relative to sphere returns.

In the field of colloid science the Mie theory is used in conjunction with experimental work to determine the particle size and concentration in dilute suspensions. However, in a few cases in this field the experiments have been carried out with the object of verifying Mie's theory; that is, the application of Equation (2-3) to explain phenomena observed when electromagnetic energy is shone on clouds of particles.

4.1 CALIBRATION PROCEDURES USING SPHERES

In this section the experimental procedures will be described somewhat more specifically, but no attempt will be made to go into details of procedure and equipment or evaluation of accuracy.

In most of the experiments the measurements are based on the

bistatic radar equation which may be written as

$$\sigma(\theta, \phi) = C \frac{P_r}{P_t} \frac{(4\pi)^3}{G_t G_r \lambda^2} R_t^2 R_r^2 , \qquad (4\text{-}1)$$

where

σ = bistatic radar cross-section of scatterer

θ, ϕ = coordinate angles defined in Figure 1

P_t = power transmitted

P_r = power received

G_t = transmitter antenna gain

G_r = receiver antenna gain

R_t = range from transmitter to scatterer

R_r = range from receiver to scatterer

λ = wavelength of radiation

C = calibration factor

For the target essentially in free space and R_t and R_r sufficiently great, C is unity. However, experimental conditions usually require one or more of these conditions to be violated, so ordinarily $C \neq 1$. In addition, the effects of experimental errors in measuring the remaining factors in Equation (4-1) may be lumped into C.

The measurement procedures are then of two types. In one type it is proposed to make absolute scattering measurements. Ranges are made

sufficiently great and the instruments needed to measure the quantities on the right of Equation (4-1) are each sufficiently accurately calibrated so that, when the quantities are measured for a sphere of known cross-section, C is acceptably close to unity. The equipment is then used to measure absolute values of σ for the scatterers of interest. This procedure was used, for example, at the Wright Air Development Center (Ref. 5) for measurement of radar cross-sections of aircraft in flight. (The calibrating sphere was hung from a balloon by a long nylon cord).

An alternative procedure not requiring such accurate calibration of the individual instruments is to measure P_r for a sphere of known $\sigma = \sigma_{sp}(\theta,\phi)$, and then to measure P_r for the scatterer of interest. Then

$$\sigma(\theta,\phi) = \sigma_{sp}(\theta,\phi) \frac{P_r(\text{with scatterer of interest})}{P_r(\text{with sphere})} \qquad (4\text{-}2)$$

This procedure is by far the more common.

In all the above, when bistatic measurements are to be made it must be remembered that σ refers to the scattered energy. Hence, it is necessary in the measurements to subtract (considering phase) the component of the primary field which enters the receiver.

A quite different experimental procedure for measuring backscattering has been used at Harvard by Aden (Ref. 1 and Ref. 2) and by Huang and Kodis (Ref. 32). This procedure makes use of the fact that the scattered and incident fields form standing waves along the path from

transmitter to scatterer. The radar cross-section can be related to the voltage standing wave ratio and position and spacing of the minima and maxima. The formula is derived in Reference 1 as

$$\sigma = 16\pi^2 \left[\frac{L\, w_2}{L-w_2}\right]^2 \left[\frac{(R_+) + \Delta/(L-w_2) - 1}{(R_+) + \dfrac{1}{1 \pm (\Delta/w_2)}}\right]^2 C$$

except that we have inserted a factor C which is considered to become closer to unity as the assumptions used previously with Equation (4-1) are more nearly satisfied. The symbols are

L = distance from scatterer to transmitter

w_2 = distance from scatterer to a chosen minimum

Δ = spacing between minimum and adjacent peaks

R_- = voltage standing wave ratio using peak adjacent to the minimum and toward the scatterer

R_+ = same as above but using peak toward transmitter

The measurement procedure used depends on symmetry about a plane and enables one to measure the quantities involved without severely disturbing the fields. The portion of the body to one side of a plane of symmetry (hemisphere, for a sphere) is placed on a conducting plane, thus simulating the entire body in free space. This method permits a receiver antenna or probe to be inserted into the field from below the plane through a small aperture with very little distortion of the field.

As a check on his set-up Aden used metal spheres of known σ to determine that C was sufficiently close to unity, then made absolute measurements of his "water spheres" (spherical shells of $n \sim 1$ filled with water). The near zone field as well as the far zone was investigated both by Huang and Kodis and by Hamren (Ref. 31).

4.2 VERIFICATION OF THE MIE THEORY

In the case of dilute suspensions of particles of uniform size, Mie's theory assumes that there is negligible interaction between particles, so that the scattering cross-section of a volume of the suspension is simply the number of particles multiplied by their individual cross-sections. It also assumes that the particles may be replaced by spheres of appropriate radius. Experimental verification of the theory is, therefore, something more than verification of Maxwell's equations. Typical examples of this verification follow.

Mie's original paper served to explain quantitatively some experimental results, found by W. Steubing, concerning the color and polarization of light scattered by gold sols. Among other things Mie pointed out that Steubing's particles indeed deviated slightly from sphericity, as indicated by the polarization at 90° scattering.

Paranpje, et al (Ref. 45) have investigated scattering as a function of the angle θ for optical scattering from an artificial aerosol

of large water droplets with ρ_a = 10, 20 and 30. They find agreement with computations based on Mie's work.

LaMer (Ref. 37) verified the use of Mie's theory in predicting the screening effect of liquid smokes. More recently Gumprecht and Sliepcevich (Ref. 29) have investigated the applicability of the Mie theory to the attenuation of intensity along a beam of light passing through a cloud of particles of large ρ_a. As ρ_a increases, more and more of the light is scattered in the forward direction.* Thus in computing attenuation due to scattering from the beam, it is necessary to use, in place of Q, the cross-section which measures the total scattered energy per particle, a cross-section, Q_a, which measures the total scattered energy minus the amount scattered forward into a small cone. The ratio $R = Q_a/Q$ is a function of the size and position in the beam of both the receiver and the particles. This dependence is experimentally investigated in Reference 29 for particles of ρ_a up to 400.

* cf References 11 and 59.

V

THEORETICAL PROCEDURES

This section was written to give theoretical support to the results given in Section II. It contains derivations of the different representations of the scattered fields and analyses of their convergence properties.

The different forms of the solution generally fall into two classes. We term those series which involve only the integral order Legendre and spherical Bessel functions the "integral order expansions", the others we shall call "complex order expansions".

5.1 DERIVATION OF INTEGRAL ORDER EXPANSIONS

Various related derivations of these expressions appear in the literature. These will be reviewed and compared here. Sources at a finite distance as well as plane incident waves will be considered. The problem is to find the $\vec{E}$ and $\vec{H}$ fields in a region external to a sphere when there is an electromagnetic wave incident on the sphere. $\vec{E}$ and $\vec{H}$ are subject to Maxwell's equations. In the region outside the sphere and excluding the source, the equations are

$$\begin{aligned} &\text{curl } \vec{E} - i\omega\mu \vec{H} = 0, \qquad &&\text{div } \vec{H} = 0 \\ &\text{curl } \vec{H} + i\omega\epsilon \vec{E} - \sigma \vec{E} = 0, \qquad &&\text{div } \vec{E} = 0. \end{aligned} \tag{5-1}$$

(We have assumed $e^{-i\omega t}$ time dependence.) In addition, the total $\vec{E}$ field has zero tangential component at the sphere surface and the scattered

field dies out like a spherical wave, i.e., satisfies the Sommerfeld radiation condition infinitely far from the sphere. If r is the distance from the sphere this condition is expressed as

$$\lim_{r \to \infty} r\left(\frac{\partial \vec{E}}{\partial r} - ik\vec{E}\right) = 0 \tag{5-2}$$

From (5-1) follows the existence of vector potentials $\vec{A}$ and $\vec{A}^*$ and scalar potentials ϕ and ϕ^* such that

$$\begin{aligned} \mu \vec{H} &= \text{curl } \vec{A} & \vec{E} &= -\text{ grad } \phi + i\omega \vec{A}, \\ \epsilon \vec{E} &= -\text{ curl } \vec{A}^*, & \vec{H} &= -\text{ grad } \phi^* + i\omega \vec{A}^*. \end{aligned} \tag{5-3}$$

A condition such as

$$\text{div grad } \phi + \mu\epsilon\omega^2 \phi = 0 \tag{5-4}$$

must be imposed on ϕ, which is otherwise arbitrary (See Chapter I of Ref. 60).

The determinations of $\vec{E}$ and $\vec{H}$ in the literature often use Hertz potentials $\vec{\Pi}$ and $\vec{\Pi}^*$, defined by

$$\vec{A} = \mu\epsilon \frac{\partial \vec{\Pi}}{\partial t}, \qquad \vec{A}^* = \mu\epsilon \frac{\partial \vec{\Pi}^*}{\partial t}, \tag{5-5}$$

or closely related functions, which will be discussed shortly. From Maxwell's equations one finds that $\vec{\Pi}$ and $\vec{\Pi}^*$ satisfy the wave equation

$$\text{curl curl } \vec{\Pi} - \text{grad div } \vec{\Pi} - \mu\epsilon\omega^2 \vec{\Pi} = 0 \tag{5-6}$$

when one lets $\phi = -\text{ div } \vec{\Pi}$, $\phi^* = -\text{ div } \vec{\Pi}^*$. Then

$$\vec{H} = -i\omega\epsilon \text{ curl } \vec{\Pi}, \qquad \vec{E} = \text{curl curl } \vec{\Pi} \tag{5-7}$$

and similarly

$$\vec{E} = \mu i\omega \operatorname{curl} \vec{\Pi}^*, \qquad \vec{H} = \operatorname{curl}\operatorname{curl} \vec{\Pi}^*. \tag{5-8}$$

The total field is the sum of those obtained from $\vec{\Pi}$ and $\vec{\Pi}^*$.

The related functions come about this way; one assumes that

$$\vec{\Pi} = \left(\frac{1}{k}\sum_{n=0}^{\infty} a_n \psi_n\right)\hat{a}, \qquad \vec{\Pi}^* = \frac{-i}{\mu\omega}\left(\sum_{n=0}^{\infty} b_n \psi_n\right)\hat{a}, \tag{5-9}$$

where $\hat{a}$ is a unit constant vector or a unit radial vector in a spherical coordinate system, and the a_n and b_n are constants. Then from (5-6) it follows that the ψ_n satisfy

$$\operatorname{curl}\operatorname{curl}\psi\hat{a} - \operatorname{grad}\operatorname{div}\psi\hat{a} - \omega^2\mu\epsilon\psi\hat{a} = 0\,.^{1} \tag{5-10}$$

One sees from (5-7) and (5-8) that

$$\vec{H} = \frac{-k}{i\mu\omega}\sum (a_n \vec{M}_n + b_n \vec{N}_n) \tag{5-11}$$

$$\vec{E} = -\sum (a_n \vec{N}_n + b_n \vec{M}_n),$$

where

$$\vec{M}_n = \operatorname{curl}\ \psi_n \hat{a}$$

$$\vec{N}_n = \frac{1}{k}\operatorname{curl}\vec{M}_n = \frac{1}{k}\operatorname{curl}\operatorname{curl}\ \psi_n \hat{a}. \tag{5-12}$$

[1] For $\hat{a}$ a constant vector, this is simply $\frac{\partial^2\psi}{\partial x^2} + \frac{\partial^2\psi}{\partial y^2} + \frac{\partial^2\psi}{\partial z^2} + \omega^2\mu\epsilon\psi = 0$.

The vectors ${}^{a}\vec{M}_n$ and ${}^{a}\vec{N}_n$ were introduced by Hansen and are termed vector wave functions. With $\hat{a} \equiv \hat{r}$, a unit radial vector, they are used as the starting point in Stratton (Ref. 60) to derive the Mie series, Equation (2-3) of Section II.

The completeness of the sets of vector wave functions (5-12) is discussed in Studies XI of this series (Ref. 55). In that report a is taken in turn to be each of the $\hat{x}$, $\hat{y}$, $\hat{z}$ unit vectors along the axes of a Cartesian coordinate system. The electromagnetic field scattered by a prolate spheroid upon which a plane wave is incident is expressed in series of certain of these resulting vectors written explicitly in terms of prolate spheroidal coordinates and the coefficients for one special ratio of major to minor axis (10:1) determined by machine computation.

When the limiting case of equal major and minor axes is taken, this prolate spheroid series gives a solution alternative to the Mie series for the sphere. The alternative series is more easily obtained directly but we have not as yet found the coefficients explicitly.

Debye wrote $\vec{\Pi}$ and $\vec{\Pi}^*$ respectively as $\vec{r}\Pi_1$ and $\vec{r}\Pi_2$. Π_1 and Π_2 are now called Debye potentials in the literature (See Ref. 9, for example, where certain advantages in the use of these potentials rather than the vector potentials $\vec{A}$ and $\vec{A}^*$ are demonstrated).

For a plane wave the expansion of the field directly in terms of ${}^{r}\vec{M}$ and ${}^{r}\vec{N}$ vectors in (5-12) is well known and leads to the Mie series in the following way: this expansion for $\vec{E}$ is added to a similar one with unknown

coefficients for the scattered field and the boundary conditions are applied to determine the coefficients. Since the boundaries are spherical, the determination is simple when the $^{r}\vec{M}$ and $^{r}\vec{N}$ type of $\vec{M}$ and $\vec{N}$ vectors are used. For a horizontal dipole source parallel to the x-axis at a finite distance from the sphere, the incident wave is most easily expanded in $^{x}\vec{M}$ and $^{x}\vec{N}$ vectors (using $\hat{a} = \hat{x}$, the unit vector in the direction of the x-axis). Tai (Ref. 61) then used relationships he derived between the two types of $\vec{M}$ and $\vec{N}$ vectors to express this incident field in terms of $^{r}\vec{M}$ and $^{r}\vec{N}$. This again makes matching the coefficients at the boundary relatively simple.

From Tai (Ref. 61) one has Equation (2-5) for the field of a horizontal dipole of moment $p\hat{x}$. The scattered field components may be written as Equation (2-6).

The a_n and b_n in Equation (2-4) are determined by the boundary conditions that

$$E^{i}_{\theta} + E^{s}_{\theta} = E^{i}_{\phi} + E^{s}_{\phi} = 0, \text{ on } r = a. \tag{5-13}$$

Note also that the condition

$$\vec{H} \cdot \vec{r} = 0 \quad \text{on } r = a \tag{5-14}$$

follows from Equation (5-13) and Maxwell's equations.

The radiation condition (5-2) is satisfied by the choice of $\zeta_n(\rho) = \sqrt{\frac{\pi\rho}{2}}\, H^{(1)}_{n+\frac{1}{2}}(\rho)$ and $\zeta'_n(\rho)$ in the expansion given in Equation (2-6)

and not by either their complex conjugates or $\psi_n(\rho)$, $\psi'_n(\rho)$, their real parts. The truth of this statement follows from the fact that the series are represented to a given accuracy by a finite number of terms, where this number, N, is independent of ρ. (This is verified in Section 5.2 after the a_n and b_n are determined*.) For now, as $\rho \to \infty$, $\rho^2 \gg N$ and therefore one can use the asymptotic form

$$\zeta_n(\rho) = (-i)^{n+1} e^{i\rho} \tag{5-15}$$

from which it is evident that the finite sum is multiplied by a factor $\frac{1}{\rho} e^{i\rho}$ and hence acts as an outgoing spherical wave to satisfy (5-2).

The conditions (5-13) may be written as

$$\begin{aligned} 0 &= \sum \frac{2n+1}{n(n+1)} \left\{ X_n \frac{P_n^1(\cos\theta)}{\sin\theta} + Y_n \frac{\partial P_n^1(\cos\theta)}{\partial \theta} \right\} \\ 0 &= \sum \frac{2n+1}{n(n+1)} \left\{ X_n \frac{\partial P_n^1(\cos\theta)}{\partial \theta} + Y_n \frac{P_n^1(\cos\theta)}{\sin\theta} \right\}, \end{aligned} \tag{5-16}$$

*Actually such a verification is carried out explicitly only for the scattering of a plane wave. However, similar considerations apply here.

where

$$X_n = \zeta_n(\rho_b)\left[\psi_n(\rho_a) + a_n \zeta_n(\rho_a)\right]$$
$$Y_n = \zeta_n'(\rho_b)\left[\psi_n'(\rho_a) + b_n \zeta_n'(\rho_a)\right] \quad . \tag{5-17}$$

By inspection one sees that (5-16) is satisfied by

$$X_n = Y_n = 0. \tag{5-18}$$

It follows from appropriate uniqueness theorems (see Reference 55) that (5-18) provides the only set of X_n and Y_n which satisfy (5-16).

There is an interesting sidelight on this statement about uniqueness which has application to the determination of coefficients for the alternate form of the solution in terms of $\vec{x}_M$, $\vec{y}_M$, and $\vec{z}_M$ vectors. Assume that the solutions (5-18) were not observed by inspection. Then a straightforward way to determine the coefficients would be to use the identity

$$\sin\theta \frac{dP_n^1(\cos\theta)}{d\theta} = \frac{n^2}{2n+1} P_{n+1}^1(\cos\theta) - \frac{(n+1)^2}{2n+1} P_{n-1}^1(\cos\theta) \tag{5-19}$$

to reduce (5-16) to expressions involving only the functions $P_n^1(\cos\theta)$ which are orthogonal over $0 \leq \theta \leq \pi$. Equating the coefficients of $P_k^1(\cos\theta)$, $k = 0, 1, \ldots$ to zero yields equations for X_n and Y_n. However, since $P_0^1 = 0$, the coefficients of P_o^1 which arise are arbitrary functions of ρ_a.

The equations are:

$$\frac{2n+3}{(n+1)(n+2)} X_{n+1} - \frac{n}{n+1} Y_n - \frac{n+3}{n+2} Y_{n-2} = 0$$

$$\frac{2n+3}{(n+1)(n+2)} Y_{n+1} + \frac{n}{n+1} X_n + \frac{n+3}{n+2} X_{n+2} = 0, \tag{5-20}$$

for $n = 0, 1, 2, \ldots$, corresponding to coefficients of $P^1_{n+1}(\cos\theta)$. Thus two coefficients appear to be arbitrary. However, there is only one choice which will yield a convergent expression. Furthermore, Equation (5-14) yields

$$X_n = 0 \qquad n = 1, 2, \ldots, \tag{5-21}$$

and no information on Y_n. However, $X_n = 0$ leaves no free choice in solving the above system of recursion equations for X_n and Y_n.

To obtain the Mie series for an incident plane wave of amplitude E_o, one lets the dipole recede toward infinity so that in the finite series $\rho_b^2 \gg N$, and (5-15) is applicable to $\zeta_n(\rho_b)$. Then letting

$$E_o = \frac{k^3 p e^{i\rho_b}}{4\pi\epsilon\rho_b} \tag{5-22}$$

in Equation (2-6) yields the Mie series.

It should be pointed out that the above solutions are also obtained by Tai in Reference 62 to illustrate use of the tensor Green's function, $\vec{\vec{G}}$, expanded in terms of $\vec{rM}$ and $\vec{rN}$ vectors. $\vec{E}$ is given by the formula

$$\vec{E} = i\omega\mu \iiint_V (\vec{J} \cdot \vec{\vec{G}})\, dv \tag{5-23}$$

derived from the vector Green's theorem. Here $\vec{J}$ is the dipole current and V is the region outside the sphere.

The convergence of these series is such that they take somewhat more than ρ_a terms to sum, which makes calculation lengthy and difficult for large ρ_a. However, alternate, more rapidly converging series have recently been obtained.

5.2 CONVERGENCE OF THE MIE SERIES

In this section an upper bound, $\overline{R}$, on the remainder of the series (2-3) after $N > \rho_a$ terms, is obtained. From this and a lower bound on the series an estimate is obtained of the number of terms needed to furnish the values of the field to a desired accuracy.

The terms to be considered are:

$$\frac{1}{\rho}\frac{2n+1}{n(n+1)}\left\{\left|\frac{\zeta_n(\rho)}{\zeta_n(\rho_a)}\right|\left|\psi_n(\rho_a)\right|\left|\frac{P_n^1(\cos\theta)}{\sin\theta}\right|+\left|\frac{\zeta'_n(\rho)}{\zeta'_n(\rho_a)}\right|\left|\psi'_n(\rho_a)\right|\left|\frac{dP_n^1(\cos\theta)}{d\theta}\right|\right\} \tag{5-24}$$

We can replace the functions of θ by $\frac{n(n+1)}{2}$, since

$$\left|\frac{P_n^1(\cos\theta)}{\sin\theta}\right| \leq \frac{n(n+1)}{2}, \qquad \theta \leq \pi \tag{5-25}$$

and

$$\left|\frac{dP_n^1(\cos\theta)}{d\theta}\right| \leq \frac{n(n+1)}{2}, \qquad \theta \leq \pi. \tag{5-26}$$

As shown in Reference 53 the first inequality may be demonstrated by induction on n by combining the facts that

$$\left|P_n(\cos\theta)\right| \leq 1, \quad P_1^1(\cos\theta) = -\sin\theta \tag{5-27}$$

and the recursion formula (Ref. 40, p. 54)

$$P_{n-1}^1(\cos\theta) - P_{n+1}^1(\cos\theta) = (2n+1)\sin\theta\, P_n(\cos\theta). \tag{5-28}$$

The second inequality (5-26) may be proven as follows. First of all,

$$\left|\frac{dP_n^1}{d\theta}\right| = \left|\frac{d^2P_n}{d\theta^2}\right| \quad . \tag{5-29}$$

Furthermore (Ref. 40, p. 50)

$$P_n(\cos\theta) = a_o \cos n\theta + a_1 \cos(n-2)\theta + \ldots + a_r \cos\theta + a_{r+1} + a_{r+2}\cos(-\theta) + \ldots + a_{r+n}\cos(-n\theta) \tag{5-30}$$

where the coefficients $a_o \ldots a_{r+n}$ are either positive functions of n or zero. Thus

$$\frac{-dP_n^2(\cos\theta)}{d\theta^2} = a_o n^2 \cos\theta + a_1(n-2)^2\cos(n-2)\theta + \ldots + a_r\cos\theta + \ldots + a_{r+n}n^2\cos(-n\theta) \tag{5-31}$$

also is the sum of cosine terms multiplied by non-negative constants. Hence

$$\left|\frac{dP_n^2(\cos\theta)}{d\theta^2}\right|$$

achieves its maximum value at $\theta = 0$. However, for a general n it is not too easy to evaluate

$$\left| \frac{d^2 P_n}{d\theta^2} \right|_{\theta = 0}$$

directly from Equation (5-30). It is simpler to use Legendre's equation which may be written in the forms

$$\frac{d^2 P_n(\cos\theta)}{d\theta^2} = x \frac{dP_n(x)}{dx} - n(n+1) P_n(x) \tag{5-32}$$

and

$$(1-x^2) \frac{d^2 P_n(x)}{dx^2} = 2x \frac{dP_n(x)}{dx} - n(n+1) P_n(x) \tag{5-33}$$

where $x = \cos\theta$. From the second form it is clear that when $\theta = 0$, i.e., $x = 1$

$$x \frac{dP_n(x)}{dx}\Bigg]_{x=1} = \frac{1}{2} n(n+1) \cdot P_n(x)\Bigg]_{x=1} = \frac{1}{2} n(n+1) \tag{5-34}$$

and hence from the form (5-32) of Legendre's equation,

$$\left| \frac{d^2 P_n}{d\theta^2} \right| \leq \frac{n(n+1)}{2} \quad . \tag{5-35}$$

Next we note that $\left| \zeta_n(\rho) \right|$ is monotone decreasing (Ref. 40, p. 25) so that

$$\frac{\left| \zeta_n(\rho) \right|}{\left| \zeta_n(\rho_a) \right|} \leq 1, \qquad \rho \geq \rho_a \tag{5-36}$$

A bound on $\dfrac{|\zeta_n'(\rho)|}{|\zeta_n'(\rho_a)|}$ may be obtained as follows: First, note that

$$\frac{d|\zeta_n'(x)|^2}{dx} = \zeta_n'\bar{\zeta}_n'' + \zeta_n''\bar{\zeta}_n' . \tag{5-37}$$

Now use the differential equation for ζ_n, namely

$$\zeta_n'' + \left(1 - \frac{n(n+1)}{x^2}\right)\zeta_n = 0, \tag{5-38}$$

to show that

$$\frac{d|\zeta_n'(x)|^2}{dx} = \frac{d|\zeta_n(x)|^2}{dx}\left(\frac{n(n+1)}{x^2} - 1\right) . \tag{5-39}$$

The first factor was shown to be negative; hence

$$\frac{d|\zeta_n'(x)|}{dx}\begin{cases} > 0, & n(n+1) < x^2 \\ < 0, & n(n-1) > x^2 . \end{cases} \tag{5-40}$$

For n fixed and $x \longrightarrow \infty$, $\zeta_n'(x) \longrightarrow 1$. The function $|\zeta_n(x)|$ looks as shown schematically in Figure 8.

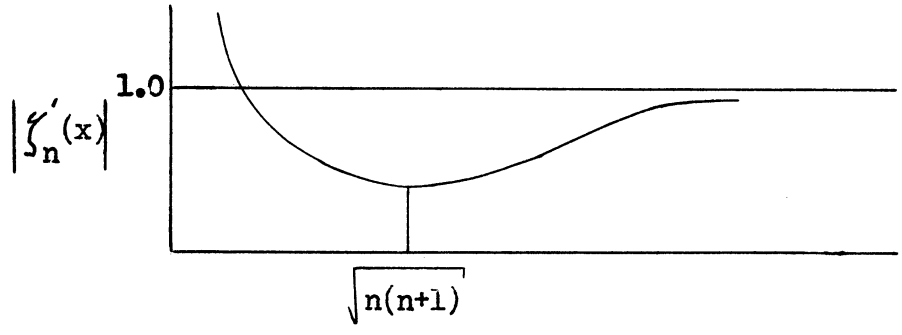

FIG. 8 SCHEMATIC REPRESENTATION OF $|\zeta_n'(x)|$

Therefore

$$\left|\frac{\zeta_n'(\rho)}{\zeta_n'(\rho_a)}\right| < 1, \quad \rho_a < \rho < \sqrt{n(n+1)} \tag{5-41}$$

and

$$\left|\frac{\zeta_n'(\rho)}{\zeta_n'(\rho_a)}\right| \leq \frac{1}{\zeta_n'(\sqrt{n(n+1)})}, \quad \rho_a < \rho \text{ and } \rho > \sqrt{n(n+1)} \tag{5-42}$$

Using the asymptotic approximation

$$H_\nu^{(1)} = \frac{\tanh\alpha}{\sqrt{3}} H_{1/3}^{(2)}\left(\frac{i\nu}{3}\tanh^3\alpha\right)\exp\left[-\nu(\tanh\alpha + \frac{1}{3}\tanh^3\alpha - \alpha) - 2i\pi/3\right] \tag{5-43}$$

with $\cosh\alpha = \nu/\rho$, we obtain

$$\left|\zeta_n'(\sqrt{n(n+1)})\right| \sim \frac{.585}{\sqrt{n(n+1)}}\left(1 - \frac{1}{4(n+\frac{1}{2})^2}\right)^{1/2} > \frac{1}{2(n+1/2)}. \tag{5-44}$$

We shall therefore make use of (5-44) to rewrite the inequality (5-42) in the form

$$\left|\frac{\zeta_n'(\rho)}{\zeta_n'(\rho_a)}\right| < 2(n+1/2) \tag{5-45}$$

It remains now to bound

$$2\,\frac{\nu^2}{\rho}\left\{\left|\psi_n(\rho_a)\right| + \left|\psi_n'(\rho_a)\right|\right\}\,, \quad \text{where } \nu = n + \tfrac{1}{2}\,.$$

From Reference 15 we have the inequality

$$\psi_\nu(\rho_a) \le \nu^{1/6}\sqrt{x}\; e^{-\nu F(0,x)} \tag{5-46}$$

where $x = \rho_a/\nu$, $0 < x \le 1$, and

$$F(0,x) = \log\left(\frac{1+\sqrt{1-x^2}}{x}\right) - \sqrt{1-x^2} \tag{5-47}$$

is shown in Figure 9. Furthermore, Watson (Ref. 69) has shown that

$$J_\nu'(\rho_a) \le \frac{(1+x^2)^{1/4}\, e^{-\nu F(0,x)}}{\sqrt{2\pi\nu}\; x}\,. \tag{5-48}$$

From this, the definition $\psi_n(y) = \sqrt{\pi y/2}\; J_{n+\frac{1}{2}}(y)$, and Eq.(5-46) we obtain

$$\psi'(\rho_a) < (\nu^{-5/6} + 2^{1/4})\,\frac{e^{-\nu F(0,x)}}{2\sqrt{x}} < \frac{3}{2}\,\frac{e^{-\nu F(0,x)}}{\sqrt{x}} \tag{5-49}$$

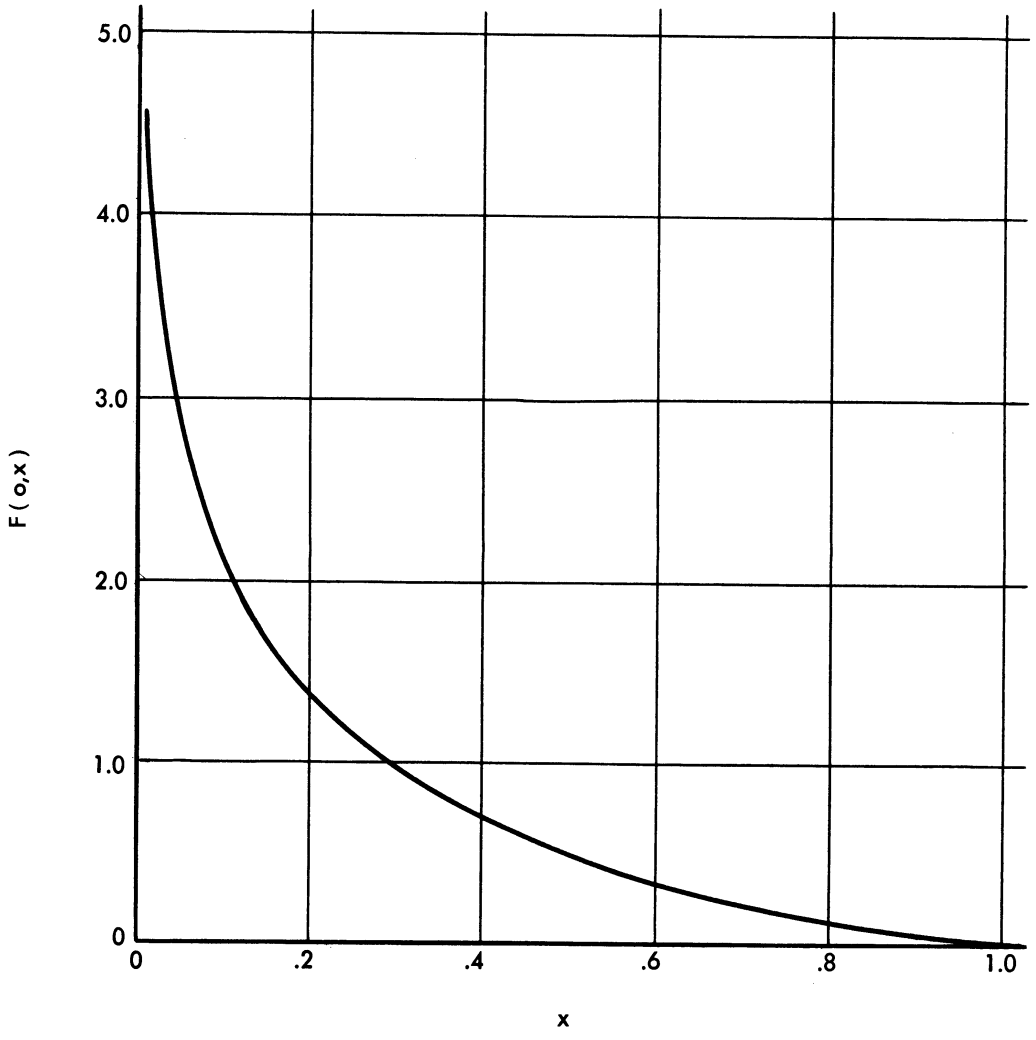

FIG. 9. AUXILIARY FUNCTION F(o,x) vs. x

Both of the bounds in (5-46) and (5-49) are bounded by

$$\frac{\nu}{\rho_a^{1/2}} \; e^{-\nu F(0,x)} \; , \nu > 3/2$$

Hence the remainder after N terms is bounded by

$$\bar{R} < \frac{4}{\rho\rho_a^{1/2}} \sum_{N+1}^{\infty} \nu^3 \, e^{-\nu F(0,\, x_{n+1})} \qquad (5\text{-}50)$$

$$= \frac{4}{\rho\rho_a^{1/2}} \frac{e^{-NF}}{(e^F - 1)^4} \left\{ e^{3F}(N+1)^3 - e^{2F}(3N^3+6N^2-4) + e^F(3N^3+3N^2+3N+1) - N^3 \right\} \equiv \bar{\bar{R}}.$$

This bound holds for the remainder in E_θ or E_ϕ. To obtain an upper bound on the error in evaluation of the sum we consider $\bar{\bar{R}}/\underline{\Sigma}$, where $\underline{\Sigma}$ is a lower bound on the sum. From numerical work available to the authors and from other considerations, it turns out that, for all θ,*

$$\underline{\Sigma} = \frac{1}{2\sqrt{10}} \; \frac{a}{r}$$

for $\rho_a > 1$.

---

* There is a possible exception for E_ϕ to this statement in a small neighborhood around $\theta \sim 120^\circ$. In this region a modified further analysis will be needed.

Where this lower bound holds we have that the relative error is less than

$$\bar{E} \equiv \frac{\bar{\bar{R}}}{\bar{\bar{\sum}}} = \frac{8\sqrt{10}}{\rho_a^{3/2}} \frac{e^{-NF}}{(e^F-1)^4} \left\{ e^{3F}(N+1)^3 - e^{2F}(3N^3+6N^2-4) + e^F(3N^3+3N^2-3N+1) - N^3 \right\} \tag{5-51}$$

where $F = F\left(0, \rho_a/(N+1)\right)$.

For any given $\bar{E}$ this relationship specifies a curve of N vs ρ_a. Figure 10 gives such a curve for $\bar{E} = .04$. For a given ρ_a, if the number of terms $N(\rho_a)$ determined from this curve is used, the relative error will be less than .04. The curve is not very sensitive to changes in $\bar{E}$.

5.3 COMPLEX ORDER EXPANSIONS

The radial vector wave functions $r\vec{M}$ and $r\vec{N}$ used in Section (2-1) are probably the most natural ones to use since they permit the boundary conditions to be satisfied in a conventional manner rather directly. However this is no reason to suspect that representations in terms of other systems of base vectors might not be more rapidly convergent. This is indeed the case, as is found in the recent literature. The rapidly convergent form given in the body of this report is essentially derived by Felsen (Ref. 17) in the course of a general treatment of acoustic and

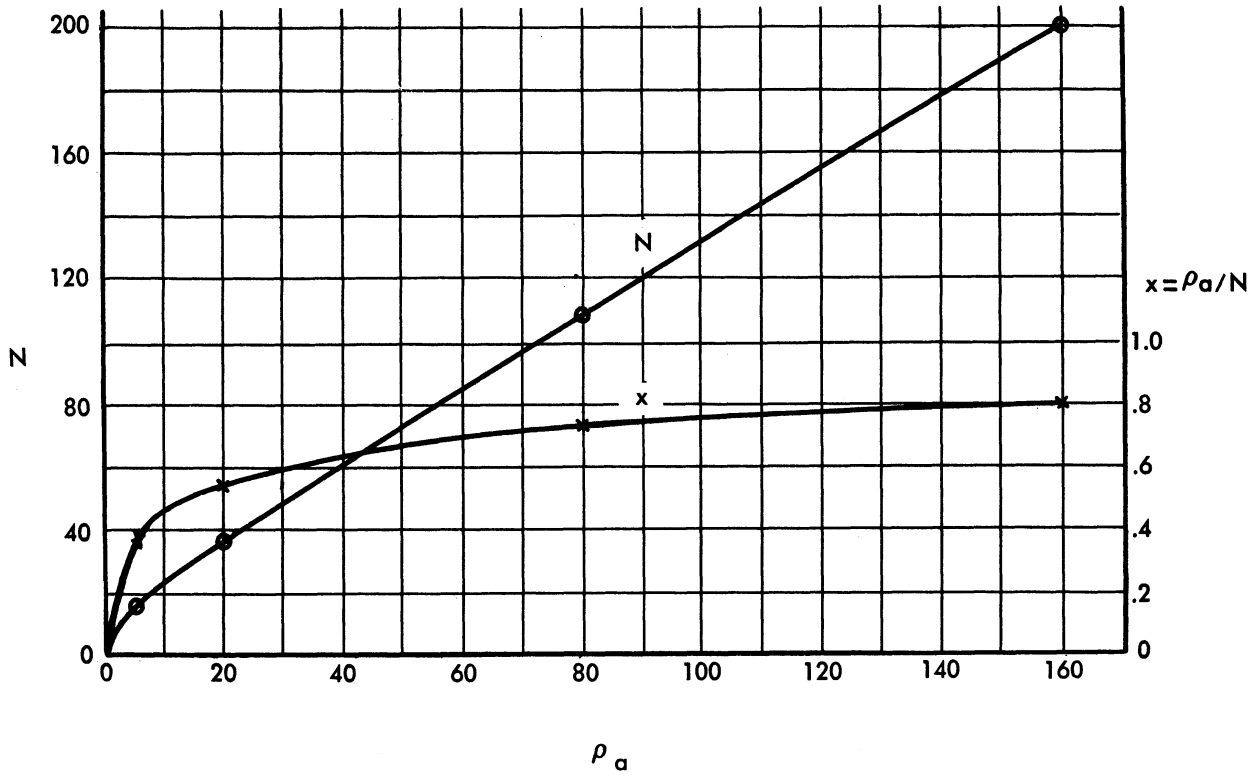

FIG. 10 NUMBER, N, OF TERMS REQUIRED IN MIE SERIES TO ASSURE 4% ACCURACY vs. ρ_a

electromagnetic problems in regions bounded by spheres, cones and planes. Using a Green's function approach, Felsen derived series* from which the Hertz potentials may be obtained by differentiation. Franz (Ref. 20), who obtains the Green's function for the vertical dipole case states that the same procedures go through for each component of the general Green's function for the sphere problem. The ideas leading to Equation (2-10) are also contained in Franz' works; however, the equation does not seem to appear explicitly there or elsewhere in the literature.

5.3.1 DERIVATION OF EQUATION(2-8)

The method used by Franz is an application of a procedure used by Watson (Ref. 69) for the vertical dipole case which, however, was carried through by him only for the dipole on the sphere's surface. It is applied to the horizontal dipole case here.

We now carry out the transformation for the θ component of the total field given by the sum of Equation (2-5) and Equation (2-6). Consider the integral

$$I = \frac{1}{2i} \int_C \frac{A_\nu \, d_\nu}{\cos(\nu\pi)}$$

* There are misprints in these series as they appear in Ref. 17. In Eqs. (4.11) and (4.15) of that reference each term should have a cos $(\phi - \phi')$ factor and in addition the factor $\frac{1}{2}$ in (4.15) should be replaced by $i/(4\pi k)$.

where

$$A_\nu = \frac{2\nu}{(\nu - \frac{1}{2})(\nu + \frac{1}{2})} \left\{ \frac{P^1_{\nu - \frac{1}{2}}(-\cos\theta)}{\sin\theta} \right.$$

$$\frac{\zeta_{\nu-\frac{1}{2}}(\rho_b)}{\zeta_{\nu-\frac{1}{2}}(\rho_a)} \left[\psi_{\nu-\frac{1}{2}}(\rho)\zeta_{\nu-\frac{1}{2}}(\rho_a) - \psi_{\nu-\frac{1}{2}}(\rho_a)\zeta_{\nu-\frac{1}{2}}(\rho) \right] \tag{5-52}$$

$$\left. + \frac{\partial P^1_{\nu-\frac{1}{2}}(-\cos\theta)}{\partial\theta} \frac{\zeta'_{\nu-\frac{1}{2}}(\rho_b)}{\zeta'_{\nu-\frac{1}{2}}(\rho_a)} \left[\psi'_{\nu-\frac{1}{2}}(\rho)\zeta'_{\nu-\frac{1}{2}}(\rho_a) - \psi'_{\nu-\frac{1}{2}}(\rho_a)\zeta'_{\nu-\frac{1}{2}}(\rho) \right] \right\},$$

and the integration is carried out in the complex ν plane about the path C consisting of the imaginary axis and a semi-circle of large radius drawn about the origin in the right half plane.

In addition to the poles at the zeros $\nu = n + \frac{1}{2}$ of $\cos\nu\pi$ there are also simple poles at the zeros $\nu = n_\ell$ of $\zeta_{\nu-\frac{1}{2}}(\rho_a)$ and $\nu = s_\ell$ of $\zeta_{\nu-\frac{1}{2}}(\rho_a)$ which lie in the first quadrant. It is assumed that the radius of the semicircle is chosen so that it does not pass over any of the poles. By the Cauchy residue theorem I equals $2\pi i$ times the sum of the residues at the poles interior to C. The sum of the residues at $\nu = (n + \frac{1}{2})$, $n = 1, 2, \ldots$ yields the series in (2-5) + (2-6). However, as shown below, direct evaluation of the integral shows that I = 0 in the limit as the

radius of the semi-circle approaches infinity. Hence, the sum of residues at $\nu = n + \frac{1}{2}$ equals minus the sum of residues at $\nu = s_\ell$ and at $\nu = n_\ell$, since the residue at $\nu = \frac{1}{2}$ can be shown to be zero. The latter two sums thus form the alternate representation of E_θ given by Equation (2-8).

The evaluation of the integral to zero will now be discussed. The analogous integral in the treatment of a non-perfect conductor does not vanish. The integrand on the imaginary axis is an odd function of ν so this part of the integral vanishes. The integral along the infinite semi-circle remains to be studied. Because the function $\zeta_\nu(\rho)$ diverges near $\left|\arg(\nu + \frac{1}{2})\right| = \frac{\pi}{2}$ for $|\nu| \gg \rho$ one has to investigate the integrand carefully in the limit as $|\nu| \to \infty$. In fact the analogous integral for the scattered field alone diverges and it is only the total field which converges as $|\nu| \to \infty$.*

We shall consider the various factors separately. For the $\psi_\nu(x)$

---

* Because of this White, (Ref. 70), who studied the scattered field for the plane incident wave case, used a completely different contour on which the integrals converged, but did not vanish. He evaluated them by stationary phase to obtain alternate representations for the scattered field which were fairly accurate for $0^\circ < \theta < 90^\circ$, and $170^\circ < \theta < 180^\circ$. See also Sec. 2.4.1 (b) on J. M. C. Scott's work.

and $\zeta_\nu(x)$ we need asymptotic forms for $J_\nu(x)$ and

$$H_\nu^{(1)}(x) = \frac{e^{-i\nu\pi} J_\nu(x) - J_{-\nu}(x)}{-i \sin \nu\pi} \tag{5-53}$$

for $|\nu| \gg x$. We have

$$J_\nu(x) \sim \left(\frac{x}{2}\right)^\nu \frac{1}{\Gamma(\nu+1)} \tag{5-54}$$

from the power series for $J_\nu(x)$. Also

$$J_{-\nu}(x) \sim \left(\frac{x}{2}\right)^{-\nu} \frac{1}{\Gamma(1-\nu)} = \left(\frac{x}{2}\right)^{-\nu} \frac{\Gamma(\nu) \sin \pi\nu}{\pi} \quad . \tag{5-55}$$

Furthermore for $|\nu| \gg 1$, $|\arg \nu| < \pi$,

$$\Gamma(\nu) \sim \sqrt{\frac{2\pi}{\nu}} \left(\frac{\nu}{e}\right)^\nu \quad . \tag{5-56}$$

With this basis we can write

$$J_\nu(\rho)\, H_\nu^{(1)}(\rho_a) \sim \frac{i}{\sin \nu\pi} \quad \frac{1}{\nu \Gamma(\nu)} \left[\frac{e^{-i\nu\pi}}{\nu\Gamma(\nu)} \left(\frac{\rho\rho_a}{4} \right)^\nu - \left(\frac{\rho}{\rho_a} \right)^\nu \frac{\Gamma(\nu)\sin\nu\pi}{\pi} \right] \tag{5-57}$$

Hence

$$J_\nu(\rho) H_\nu^{(1)}(\rho_a) - J_\nu(\rho_a) H_\nu^{(1)}(\rho) \sim \frac{i}{\nu\pi} \left[\left(\frac{\rho}{\rho_a} \right)^\nu - \left(\frac{\rho_a}{\rho} \right)^\nu \right] . \tag{5-58}$$

Next we shall consider the ratio

$$\frac{H_\nu^{(1)}(\rho_b)}{H_\nu^{(1)}(\rho_a)} .$$

For this purpose use Equations (5-53) to (5-56) to find that

$$H_\nu^{(1)}(x) \sim -i \sqrt{\frac{2}{\pi\nu}} \left[\left(\frac{2\nu}{ex} \right)^\nu - \frac{e^{-i\nu\pi}}{2 \sin \nu\pi} \left(\frac{xe}{2\nu} \right)^\nu \right] . \tag{5-59}$$

We shall write $\nu = \nu_r + i\nu_i = |\nu| e^{i\psi}$. Note that

$$\left(\frac{2\nu}{ex} \right)^\nu = \exp \left[\nu_r \log \frac{2|\nu|}{ex} - \nu_i \psi + i \left(\nu_i \log \frac{2|\nu|}{ex} + \nu_r \psi \right) \right] \equiv \exp(a+ib) \tag{5-60}$$

$$\frac{e^{-i\nu\pi}}{2\sin\nu\pi}\left(\frac{xe}{2\nu}\right)^{\nu} = -\frac{i\nu_i}{|\nu_i|}\exp\left\{-a+(\nu_i-|\nu_i|)\pi - i\left[b+(\nu_r-\frac{\nu_i}{|\nu|}\nu_r)\pi\right]\right\}$$

The two terms in Eq. (5-59) have the same magnitude for $|\nu| \gg 1$, $x<\nu$ and $-\frac{\pi}{2} < \psi < \frac{\pi}{2}$ for one ψ only, namely

$$\psi_b(|\nu|, x) \cong \frac{\pi}{2}\,\frac{\log\left[\frac{2|\nu|}{ex}\right]}{1+\log\left[\frac{2|\nu|}{ex}\right]} \quad . \tag{5-61}$$

When $\psi = \psi_b$, $\left|H_\nu^{(1)}(x)\right| = 2\sqrt{\frac{2}{\pi\nu}}\sin(b+\frac{\pi}{4})$. The zeros of $H_\nu(x)$ (and hence the poles, ν_ℓ (ρ_a), of the integrand) lie along the curve defined by $\sin\left[b(\rho_a)+\pi/4\right] = 0$ in the ν plane. Also note that

$$\frac{\partial \psi_b(|\nu|,x)}{\partial x} \sim \frac{x}{\log|\nu|}$$

so that $\psi_b(|\nu|,\rho_b) > \psi_b(|\nu|,\rho_a)$ and for sufficiently large $|\nu|$, $\psi_b(|\nu|,\rho_b) \sim \psi_b(|\nu|,\rho_a)$.

We shall consider separately three cases (a), (b), and (c) corresponding respectively to the first term dominating in the $H_\nu(\rho_a)$, $H_\nu(\rho_b)$, to both terms of the same order of magnitude, and to the second

term dominating. In case (b) we recall that the path of integration avoids the poles $\nu_\ell\,(\rho_a)$ and in fact we can route it through the region for which $\sin\left[\, b(\rho_a) + \frac{\pi}{4}\right] \sim 1$. Then we can write

$$\left|\frac{H_\nu^{(1)}(\rho_b)}{H_\nu^{(1)}(\rho_a)}\right| = \begin{cases} \left(\dfrac{\rho_a}{\rho_b}\right)^{\nu_r} & \text{(a)} \\ (\lesssim)\ 1 & \text{(b)} \\ \left(\dfrac{\rho_b}{\rho_a}\right)^{\nu_r} & \text{(c)} \end{cases} \tag{5-62}$$

For the Legendre function $P^1_{\nu-\frac{1}{2}}(-\cos\theta)$ we use the asymptotic form

$$P^1_{\nu-\frac{1}{2}}(-\cos\theta) = \sqrt{\frac{2}{\pi\sin\theta}}\sqrt{\nu}\,\cos\left[\,(\nu+\tfrac{1}{2})(\pi-\theta)+\frac{\pi}{4}\right] \tag{5-63}$$

which is valid for $|\nu| \gg 1$ and $\pi - \dfrac{1}{|\nu|} \gg \theta \gg \dfrac{1}{|\nu|}$. Thus we have the ν dependence

$$\left|\frac{1}{\cos\nu\pi}\;P^1_{\nu-\frac{1}{2}}(-\cos\theta)\right| \sim c'\exp\left\{\tfrac{1}{2}\log|\nu| + |\nu_i|\;(\pi-\theta) - |\nu_i|\,\pi\right\}$$
$$= c'\exp\left\{\tfrac{1}{2}\log|\nu| - |\nu_i|\;\theta\right\} \tag{5-64}$$

where c' is of the order of unity.

Finally, using $d\nu = |\nu| d\psi$, we have the following bounds for the magnitude of the first half of the integrand for large $|\nu|$ in cases (a), (b) and (c) respectively:

$$\left| \frac{\nu |\nu|}{(\nu - \frac{1}{2})(\nu + \frac{1}{2})} \frac{P^1_{\nu - \frac{1}{2}}(-\cos\theta)}{\cos \nu\pi} \frac{\zeta_\nu(\rho_b)}{\zeta_\nu(\rho_a)} \left[\zeta_\nu(\rho_a)\, \psi_\nu(\rho) - \zeta_\nu(\rho)\, \psi_\nu(\rho_a) \right] \right|$$

$$\leq \left\{ \begin{array}{l} \left(\frac{\rho}{\rho_b}\right)^{\nu_r} \\ \left(\frac{\rho}{\rho_a}\right)^{\nu_r} \\ \left(\frac{\rho_b}{\rho_a^2}\right)^{\nu_r} \end{array} \right\} \cdot \quad c'' \exp\left\{ -\tfrac{1}{2} \log|\nu| - |\nu_i|\, \theta \right\} \qquad \begin{array}{l} \text{(a)} \\ \text{(b)} \\ \text{(c)} \end{array} \qquad (5\text{-}65)$$

where c'' is the order of unity.

Recalling that $\rho_b > \rho > \rho_a$ and that $\nu = n + \frac{1}{2}$ is avoided by the path of integration it is clear that the integrand vanishes as $|\nu| \longrightarrow \infty$ in the first case. It does not vanish in cases (b) and (c).

Let us determine an angle $\psi = \psi_o$ such that for $\psi < \psi_o$ case (a) clearly holds. For $\psi > \psi_o$ we shall then use the ν dependence given by case (c) and evaluate the portion of the line integral from $\psi = \psi_o$ to $\psi = \frac{\pi}{2}$.

We accordingly specify a number y such that $e^{2y} \ll 1$. Then for $a(|\nu|, \psi, \rho_a) \leq y$ case (a) holds. We can therefore determine ψ_o from the relation $a(|\nu|, \psi_o, \rho_a) = y$, i.e.,

$$|y| = |\nu| \left(\log \frac{2|\nu|}{e\rho_a} \cos \psi_o - \psi_o \sin \psi_o\right) .$$

This yields

$$\psi_o \sim \frac{\pi}{2} \frac{\log \frac{2|\nu|}{e\rho_a} - \frac{2|y|}{\pi|\nu|}}{\log \frac{2|\nu|}{e\rho_a} + 1} . \tag{5-66}$$

The contribution to the integral for $\psi_o < \psi < \frac{\pi}{2}$ is bounded above by

$$c'' e^{-\frac{1}{2}\log|\nu|} \int_{\psi_o}^{\pi/2} \exp\left[-\theta|\nu| \sin\psi + |\nu| \cos\psi \log\left(\frac{\rho\rho_b}{\rho_a^2}\right)\right] d\psi$$

$$\leq c''\left(\frac{\pi}{2} - \psi_o\right) \exp\left[-\tfrac{1}{2}\log|\nu| + |\nu|\left(-\theta \sin\psi_o + \cos\psi_o \log\left(\frac{\rho\rho_b}{\rho_a^2}\right)\right)\right] \tag{5-67}$$

Since $\theta > 0$ it follows from Eq. (66) that this bound vanishes in the

limit as $|\nu|$ increases. The magnitude of the second half of the integrand turns out to behave like this $|\nu|^2$ times the first half. Hence the integral I equals zero.

The analogous integrals for E_ϕ and for the case where $\rho > \rho_b$ are handled in the same way; all have the same exponential dependence on the semi-circle as $|\nu| \to \infty$.

5.3.2 Rapidity of Convergence of Equation (2-8)

The complex order series (2-8) may be shown to converge for all $\theta > 0$, the magnitude of the terms going, for large enough ℓ, essentially as e^{-t_ℓ} where $t_\ell \ln t_\ell \sim \ell\pi$. The early terms, however, increase with ℓ when the observation point is not in the geometric shadow region, these terms decreasing "rapidly" only within a certain limited region of the shadow. It is the purpose of this section to determine this region for a particular definition of "decreasing rapidly". Before making such a definition, we first discuss some general aspects of the series.

Approximate formulas for the zeroes, s_ℓ and n_ℓ, are available for small and for very large ℓ; those for small ℓ, in the "tangent approximation* are

* The formulas for the zeroes of ζ_ν and ζ_ν' used here arise from the so-called "tangent approximation", those of Equation (2-9) from the "Hankel approximation". This terminology is used in Bremmer's book (Ref. 10, p 36).

$$n_\ell \simeq \rho_a + \frac{1}{2}\, e^{i\pi/3} \rho_a^{1/3} \left[\frac{3\pi}{4}(4\ell - 1)\right]^{2/3}$$

$$s_\ell \simeq \rho_a + \frac{1}{2}\, e^{i\pi/3} \rho_a^{1/3} \left[\frac{3\pi}{4}(4\ell - 3)\right]^{2/3} \qquad (5\text{-}68)$$

these being valid up to larger and larger values of ℓ the greater ρ_a is. (The maximum value of ℓ is linear in ρ_a). In this range of ℓ, the magnitudes of the terms S_ℓ and N_ℓ in the series (S_ℓ and N_ℓ involve s_ℓ and n_ℓ respectively) decrease monotonically within the shadow region. Hence we feel that in a reasonable definition of "rapid convergence", a necessary condition is that the ratios $\left|S_2/S_1\right|$ and $\left|N_2/N_1\right|$ be small. A sufficient condition would involve an investigation of those intermediate values for which the above approximations cease to be good, requiring that the corresponding terms contribute negligibly to the sum. Although it is felt to be highly probable that the intermediate and higher terms are negligible when the early terms decrease rapidly, it would be desirable to prove this; (we have not carried out such a proof). In this section we will determine the region (in r,θ) within which $\left|S_2/S_1\right| \leq \eta$ and $\left|N_2/N_1\right| \leq \eta$ (η is some fixed small number).

We will use the following asymptotic expressions, wherein $\nu = \nu^r + i\nu^i$ stands for either n_ℓ or s_ℓ,

$$\left.\begin{aligned} \left|\zeta_\nu(\rho)\right| &\cong e^{-\nu i \cos^{-1}(\rho_a/\rho)} \\ \left|\zeta_\nu'(\rho)\right| &\cong \left|\zeta_\nu(\rho)\right| \end{aligned}\right\} \quad \text{Debye approximation} \qquad (5\text{-}69a)$$

$$\left.\begin{aligned} \left|\psi_\nu(\rho_a)\right| &\cong \left(\frac{\sqrt{3}\,\rho_a}{4\nu^i}\right)^{1/4} \\ \left|\psi_\nu'(\rho_a)\right| &\cong \rho_a \left(\frac{4\nu^i}{\sqrt{3}\,\rho_a}\right)^{1/4} \\ \left|\frac{\partial}{\partial\nu}\,\zeta_\nu(\rho_a)\right| &\cong 2\left(\frac{4\nu^i}{\sqrt{3}\,\rho_a}\right)^{1/4} \\ \left|\frac{\partial}{\partial\nu}\,\zeta_\nu'(\rho_a)\right| &\cong 2\left(\frac{4\nu^i}{\sqrt{3}\,\rho_a}\right)^{3/4} \end{aligned}\right\} \quad \begin{array}{l}\text{Tangent} \\ \text{Approximation} \\ \\ (5\text{-}69b)\end{array}$$

$$\left.\begin{aligned} \left|P_\nu^1(-\cos\theta)\right| &\cong \sqrt{\frac{1}{2\pi\sin\theta}}\,|\nu|^{1/2}\, e^{\nu i|\pi-\theta|} \\ \left|\frac{\partial P_\nu^1(-\cos\theta)}{\partial\theta}\right| &\cong \sqrt{\frac{1}{2\pi\sin\theta}}\,|\nu|^{3/2}\, e^{\nu i|\pi-\theta|} \end{aligned}\right\},\ \frac{\pi}{2} > \pi-\theta \gtrsim \frac{1}{\rho_a^{1/3}}\ , \tag{5-69c}$$

and the exact formulae

$$\left[\frac{P_\nu^1(-\cos\theta)}{\theta}\right]_{\theta=\pi} = -\left[\frac{\partial P_\nu^1(-\cos\theta)}{\partial\theta}\right]_{\theta=\pi} = -\frac{\nu(\nu+1)}{2}\ , \tag{5-70}$$

From these one may see that $|N_\ell| << |S_\ell|$ and $|N_{\ell+1}/N_\ell| \approx |S_{\ell+1}/S_\ell|$, at least for fairly small ℓ, when $(\rho_b - \rho_a) >> \rho_a^{1/3}$ and the observation point is in that part of the shadow region for which $\pi - \theta > 1/\rho_a^{1/3}$ or $\theta = \pi$ and $(\rho - \rho_a) >> \rho_a^{1/3}$. Hence we need consider only the ratio

$$\Lambda \equiv \left|\frac{S_2}{S_1}\right| \tag{5-71}$$

Using (5-69) and (5-70) we obtain

$$\Lambda \cong \left|\frac{s_2}{s_1}\right|^{1/2}\left(\frac{1}{5}\right)^{1/3} \exp\left[-(s_2^i - s_1^i)\left(\theta - \cos^{-1}\frac{\rho_a}{\rho} - \cos^{-1}\frac{\rho_a}{\rho_b}\right)\right], \pi-\theta > \frac{1}{\rho_a^{1/3}}$$

(5-72)

$$\Lambda = \left|\frac{s_2}{s_1}\right|\left(\frac{1}{5}\right)^{1/3} \exp\left[-(s_2^i - s_1^i)\left(\pi - \cos^{-1}\frac{\rho_a}{\rho} - \cos^{-1}\frac{\rho_a}{\rho_b}\right)\right],\ \theta = \pi\ .$$

The factors multiplying the exponential are both $\cong .6$.

Then, if we denote $s_2^i - s_1^i$ by s_{12}^i and require $\wedge \leq \eta \leq 1/2$, we obtain (to within our approximations) that

$$\frac{\rho_a}{\rho} \geqslant \cos(\theta - \theta_1 - \delta), \qquad (5\text{-}73)$$

where

$$\delta = \frac{1}{s_{12}^i} \ln\left(\frac{0.6}{\eta}\right) \text{rad.; and } \theta_1 = \cos^{-1}\left(\frac{\rho_a}{\rho_b}\right).$$

Inequality (5-73) is valid for $\theta = \pi$ and $\left(\frac{1}{\rho_a}\right)^{1/3} < \theta < \pi - \left(\frac{1}{\rho_a}\right)^{1/3}$.

The geometrical significance of these results can be seen from the fact that $\cos^{-1}(a/r) = \theta - \theta_1 - \delta$ is the equation of a cone, the generators of which are perpendicular to those of the cone $\theta = \theta_1 + \delta$, and are tangent to the sphere. This is shown in Figure 11, the region $r < r_o$ being excluded since the approximations made in using the Debye expansions

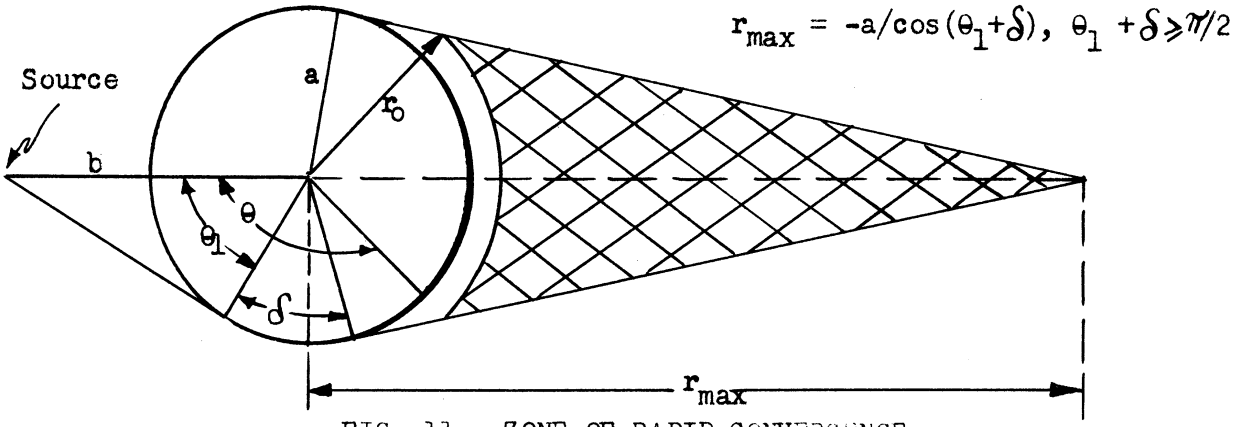

FIG. 11 ZONE OF RAPID CONVERGENCE

for the Hankel function required $(\rho - \rho_a) >> (\rho_a)^{1/3}$. Note that r_{max} may be infinite; this occurs when $\theta_1 + \delta \leq \frac{\pi}{2}$. In other words when $\theta_1 + \delta \leq \frac{\pi}{2}$ and $\theta \geq \frac{\pi}{2} + \theta_1 + \delta$, then $\Lambda \leq \eta$ for all r.* In the case $r_b \longrightarrow \infty$ (incident plane wave), we see that r_{max} is finite for all η (assuming $\eta < .1$).

A numerical example will help to give a feeling for the magnitudes involved when ρ_a is large but much less than the ρ_a encountered in radio propagation around the earth (where ρ_a's exceed 1000). We shall consider $64 \leq \rho_a \leq 125$, $\rho_a = 64$ being down to a range where the asymptotic forms used begin to be poor approximations. Then, since

$$s_{12}^{i} \simeq 1.5\, \rho_a^{1/3}$$

s_{12}^{i} lies between 6.0 and 7.5. Thus for $\eta = .06$ ($\Lambda < 0.1$), δ is approximately between 22° and 18°. Λ (in the sense of the average mentioned previously) is approximately .06 on the surfaces of the cones corresponding to these δ's and the given ρ_b. For an incident plane wave, we find that r_{max}/a is between 2.7 and 3.2.

---

* These statements have not been proved for $\pi - 1/\rho_a^{1/3} < \theta < \pi$ since one of the terms in the cosine appearing in the approximation to $P_\nu^{(1)}(-\cos\theta)$ has been neglected. In this region, both terms become comparable, corresponding physically to the interaction between waves traveling around the sphere in opposite directions. Λ can be expected to oscillate with θ on the surface of the cone in this region, so that η is a kind of average of Λ.

5.4 REPRESENTATION USEFUL IN THE IRRADIATED REGION

It is evident from the preceding section that the series 2-8 is slowly convergent except well within the shadow region. That is, only there do the terms of the series decrease rapidly from the beginning. It is obviously of interest to obtain an expression which is useful in the directly irradiated region.

For this purpose we introduce partitions of the Legendre function and its derivative which are analogous to those used, for example, by Franz for the vertical dipole and for the cylinder case. The technique is to split from the series a term which contains the geometric optics scattered field. The remaining series converges rapidly in the lighted region. Prior motivation for this type of partition other than analogy with Franz will be discussed at the end of this section. The partition consists in writing

$$P_\nu^1(-\cos\theta) = -e^{i\nu\pi} P_\nu^1(\cos\theta) + 2i \sin\nu\pi\, G_\nu(\theta)$$

where $G_\nu(\theta) = \frac{P_\nu^1(\cos\theta)}{2} + \frac{1}{i\pi} Q_\nu^1(\cos\theta)$, *

and $Q_\nu^1(\cos\theta)$ is the Associated Legendre function of the second kind.

We introduce the partition expressions into Equation 2-8, and obtain $E_\theta = S_1 + S_2$ where

$$S_1 = \frac{ik^3 p\cos\phi}{4\epsilon\rho\rho_b} \sum_{\ell=1} \left[\frac{(2n_\ell + 1)}{n_\ell(n_\ell+1)} \frac{e^{in_\ell\pi}}{\sin n_\ell\pi} \frac{P_{n_\ell}^1(\cos\theta)}{\sin\theta} \frac{\zeta_{n_\ell}(\rho)\zeta_{n_\ell}(\rho_b)\psi_{n_\ell}(\rho_a)}{\frac{\partial}{\partial n}\zeta_n(\rho_a)}\Big|_{n=n_\ell} \right.$$

$$\left. + \frac{(2s_\ell + 1)}{s_\ell(s_\ell+1)} \frac{e^{is_\ell\pi}}{\sin s_\ell\pi} \frac{\partial P_{s_\ell}^1(\cos\theta)}{\partial\theta} \frac{\zeta'_{s_\ell}(\rho_b)\zeta_{s_\ell}(\rho)\psi'_{s_\ell}(\rho)}{\frac{\partial}{\partial s}\zeta_s(\rho_a)}\Big|_{s=s_\ell} \right]$$

and

$$S_2 = \frac{k^3 p\cos\phi}{2\epsilon\rho\rho_b} \sum_{\ell=1} \left[\frac{(2n_\ell + 1)}{n_\ell(n_\ell+1)} \frac{G_{n_\ell}(\cos\theta)}{\sin\theta} \frac{\zeta_{n_\ell}(\rho)\zeta_{n_\ell}(\rho_b)\psi_{n_\ell}(\rho_a)}{\frac{\partial}{\partial n}\zeta_n(\rho_a)}\Big|_{n=n_\ell} \right.$$

$$\left. + \frac{(2s_\ell + 1)}{s_\ell(s_\ell+1)} \frac{\partial G_{s_\ell}(\theta)}{\partial\theta} \frac{\zeta'_{s_\ell}(\rho)\zeta'_{s_\ell}(\rho_b)\psi'_{s_\ell}(\rho_a)}{\frac{\partial}{\partial s}\zeta'_s(\rho_a)}\Big|_{s=s_\ell} \right]$$

* See Reference 40 Pg. 63.

Where before convergence was governed by the form $\theta - \theta_1 - \cos^{-1}\frac{\rho_a}{\rho}$, the convergence of S_1 is now determined by $\theta - 2\pi + \theta_1 + \cos^{-1}\frac{\rho_a}{\rho}$. Rapid convergence is, therefore, obtained for S_1 in the irradiated region.

S_2 can be written as integrals over contours surrounding the points n_ℓ and s_ℓ respectively, excluding $\nu = 0$ and $\nu = -1$. Noting that the integrals over the semicircle in the upper half plane vanish, we find that

$$S_2 = \frac{k^3 p\cos\phi}{2\pi i \epsilon \rho \rho_b}(I + K)$$

where

$$I = \frac{1}{\sin\theta}\int_C d\mu \frac{\mu}{\mu^2 - \frac{1}{4}} G_{\mu-\frac{1}{2}}(\theta) \frac{\zeta_{\mu-\frac{1}{2}}(\rho_b)}{\zeta_{\mu-\frac{1}{2}}(\rho_a)}\left[\zeta_{\mu-\frac{1}{2}}(\rho)\psi_{\mu-\frac{1}{2}}(\rho_a) - \zeta_{\mu-\frac{1}{2}}(\rho_a)\psi_{\mu-\frac{1}{2}}(\rho)\right]$$

$$K = \int_C d\mu \frac{\mu}{\mu^2 - \frac{1}{4}} G'_{\mu-\frac{1}{2}}(\theta) \frac{\zeta'_{\mu-\frac{1}{2}}(\rho_b)}{\zeta'_{\mu-\frac{1}{2}}(\rho_a)}\left[\zeta'_{\mu-\frac{1}{2}}(\rho)\psi'_{\mu-\frac{1}{2}}(\rho_a) - \zeta'_{\mu-\frac{1}{2}}(\rho_a)\psi'_{\mu-\frac{1}{2}}(\rho)\right],$$

and the contour C is shown in Figure 2.

For $1 << \rho_a << \rho << \rho_b$, I and K may be approximated by a saddle point evaluation. The result of this evaluation is to show that K approaches the sum of the geometric optics scattered field and the incident field. The saddle point for the first terms of I and K occurs at $\mu_1 \cong \rho_a \sin\frac{\theta}{2}$, that for the second terms at $\mu_2 = \sin\theta$. Due to the derivative of $G_{\mu-\frac{1}{2}}(\theta)$ occurring in K, the latter is a factor of ρ_a larger than I.

Thus this partition which was chosen purely by analogy to the one used by Franz does result in having the s olution as the sum of a rapidly convergent series plus a term which contains the geometric optics scattered field and the incident field. However, it is not clear how Franz was guided to make this partition. Such a partition is obviously not unique, and to obtain the first correction, for large ρ_a, to the geometric optics answer, one must compare the first terms of the series (S_1) with the higher order terms obtained in the saddle point evaluation of S_2.

It is interesting to note that in the cylinder problem (where the lack of an evident guide to Franz' partition is also present) Friedlander's approach leads him quite naturally to a partition into the reflected field (plus incident field) and the field due to the passage

of energy around the body. The obvious question now is, are the partitions of Franz and Friedlander the same? We shall show the answer to be yes. Friedlander's solution is of the form

$$G = \sum_{n=-\infty}^{\infty} F(\theta + 2n\pi)$$

where

$$F(\theta) = -\frac{\pi}{2} \sum_{\ell=1}^{\infty} K_\ell \, e^{i\nu_\ell |\theta|}, \quad -\infty < \theta < \infty$$

(see Section 2.5). Limiting ourselves to $0 \leq \theta \leq \pi$, it follows from the discussion in Section 2.5 that $F(\theta)$, for θ in the lighted region, is exactly the field due to the geometrically reflected wave front plus the incident field. Thus the natural partition is

$$G = F(\theta) + G' \quad , \quad 0 \leq \theta < \pi, \ \theta \text{ in the lighted region.}$$

Then $$G' = \sum_{n=1}^{\infty} F(\theta + 2n\pi) + \sum_{n=1}^{\infty} F(\theta - 2n\pi)$$

$$= -\frac{\pi}{2} \sum_{n=1}^{\infty} \sum_{\ell=1}^{\infty} K_\ell \left(e^{i\nu_\ell(\theta + 2n\pi)} + e^{i\nu_\ell(\theta - 2n\pi)} \right)$$

But $|\theta - 2n\pi| = 2n\pi - \theta$ for $n \geq 1$, $\theta < \pi$.

Hence

$$G' = -\pi \sum_{n=1}^{\infty} \sum_{\ell=1}^{\infty} K_\ell \, e^{2i\nu_\ell \pi n} \cos \nu_\ell \theta = -\pi \sum_{\ell=1}^{\infty} K_\ell \frac{e^{2i\pi\nu_\ell}}{1-e^{2i\pi\nu_\ell}} \cos \nu_\ell \theta$$

$$= \frac{i\pi}{2} \sum_{\ell=1}^{\infty} K_\ell \frac{e^{i\pi\nu_\ell} \cos \nu_\ell \theta}{\sin \nu_\ell \pi} \quad ,$$

which is identical to Franz' partition.

ACKNOWLEDGEMENTS

We wish to acknowledge the cooperation of various people in helping the authors accumulate the information presented in this report and for their parts in discussions of theoretical questions; namely N. Logan and R. Penndorf of Air Force Cambridge Research Center, R. Kodis, S. Rubinow and T. T. Wu of Harvard, R. G. Kell of the Cornell Aeronautical Laboratory, Inc., and many members of the Theory and Analysis Department of the Engineering Research Institute, The University of Michigan.

REFERENCES

1. A. L. Aden, "Electromagnetic Scattering From Spheres with Sizes Comparable to a Wavelength", Journal of Applied Physics, 22, 601 (1951).

2. _____, "Back-scattering of Electromagnetic Waves from Spheres and Spherical Shells", Geophysical Research Paper No. 15, Geophysics Research Division, Air Force Cambridge Research Center, (July 1952).

3. A. L. Aden and M. Kerker, "Scattering of Electromagnetic Waves for Two Concentric Spheres", Journal of Applied Physics, 22, (Oct. 1951).

4. R. V. Alred, "Scattering of Electromagnetic Waves by Metallic Spheres Covered with Absorbing Materials", Report XRE 4/47/5. Admiralty Signal Establishment, Witley, Surrey, England (22 Dec. 1947).

5. W. F. Bahret, "Dynamic Measurements of Aircraft Radar Reflection Characteristics, Part I, Measurement Equipment and Techniques", Technical Report 53-148, Wright Air Development Center, (Apr. 1953).

6. J. D. Bain, "Radiation Pattern Measurements of Stub and Slot Antennas on Spheres and Cylinders", Technical Report No. 42, Contract No. AF19(640)-266, Stanford Research Institute, (April 1953).

7. H. Blumer, "Strahlungsdiagramme kleiner dielektrischen Kugeln", Zeitschrift für Physik, 32, 119-134 (1925).

8. C. J. Bouwkamp, "Diffraction Theory", Reports on Progress in Physics, 17, pp. 35-100 (1954).

9. C. J. Bouwkamp and H. B. G. Casimir, "On Multipole Expansions in the Theory of Electromagnetic Radiation", Physica, XX, pp. 539-554 (1954).

10. H. Bremmer, Terrestrial Radio Waves, Elsevier Publishing Company, New York (1949).

11. L. Brillouin, "Scattering Cross-Section of Spheres for Electromagnetic Waves", Journal of Applied Physics, 20, 1110-1125 (1949).

12. Chiao-Min Chu, "Scattering and Absorption of Water Droplets at Millimeter Wavelengths", Thesis (EE Dept.), The University of Michigan, (1952).

13. Chiao-Min Chu and S. W. Churchill, "Representation of the Angular Distribution of Radiation Scattered by a Spherical Particle", Journal of the Optical Society of America, 45, 958-962, (Nov. 1955).

14. S. B. Cohn and T. Morita, "Microwave Radiation from Large Finite Bodies", Technical Report 48, AF19(604)-1296, Stanford Research Institute, (Jan. 1955).

15. T. B. Curtz and K. M. Siegel, "Inequalities Involving Cylindrical Functions", Proceedings of the American Mathematical Society, 6, pp 823-827, (Oct. 1955).

16. P. Debye, "Der Lichtdruck auf Kugeln von beliebigem Material", Annalen der Physik, 30, 57-136, (1909).

17. L. B. Felsen, "Alternative Field Representations in Regions Bounded by Spheres, Cones and Planes", Research Report R-359-54, PIB-293, Polytechnic Institute of Brooklyn, (Jan. 1954).

18. V. A. Fock, "Diffraction of Radiowaves Around the Earth's Surface", Publishers of the Academy of Sciences, USSR, (1946). (Translation by Morris D. Friedman).

19. _____, "The Distribution of Currents Induced by a Plane Wave on the Surface of a Conductor", Journal of Physics, X, No. 2, p 130, (1946).

20. W. Franz, "Über die Greenschen Funktionen des Zylinders und der Kugel", Zeitschrift für Naturforschung, 9a, 705-716, (1954).

21. W. Franz and P. Beckmann, "Creeping Waves for Objects of Finite Conductivity", Proceedings of the Symposium on Electromagnetic Wave Theory, Institute of Radio Engineers Transactions, AP-4, No. 3, (July 1956).

22. F. Friedlander, "Diffraction of Pulses by a Circular Cylinder", Research Report No. EM-64, Contract No. AF19(122)-42, Institute of Mathematical Sciences, Division of Electromagnetic Research, New York University, (April 1954).

23. _____, "Note on the Geometrical Optics of Diffracted Wave Fronts", Proceedings of the Cambridge Philosophical Society, 45, p 345, (1949).

24. B. Friedman, "Propagation in a Non-homogeneous Atmosphere", Symposium on Theory of Electromagnetic Waves, pp 317-350, Interscience Publishers, New York, (1951).

25. F. T. Gucker and S. B. Cohn, "Numerical Evaluation of the Mie Scattering Functions π_n and τ_n of Orders 1 to 32 at 2.5° Intervals", Journal of Colloid Science, 8, pp. 555-574 (1953).

26. R. O. Gumprecht and C. M. Sliepcevich, Tables of Functions of First and Second Partial Derivatives of Legendre Polynomials, Engineering Research Institute, The University of Michigan (1951).

27. _____, Tables of Ricatti Functions for Large Arguments and Orders, Engineering Research Institute, The University of Michigan (1951).

28. _____, Tables of Light-Scattering Functions for Spherical Particles, Engineering Research Institute, The University of Michigan (1951).

29. _____, "Scattering of Light by Large Spherical Particles", Journal of Physical Chemistry, 57, p. 90 (1953).

30. R. O. Gumprecht, Neng-Lun Sung, Jen H. Chin, C. M. Sliepcevich, "Angular Distributions of Intensity of Light Scattered by Large Droplets of Water", Journal of the Optical Society of America, 42, p. 226 (1952).

31. S. D. Hamren, "Scattering From Spheres", University of California, Antenna Laboratory, Report No. 171, (June 15, 1950).

32. C. Huang and R. D. Kodis, "Diffraction by Spheres and Edges at 1.25 Centimeters", Technical Report No. 138, Cruft Laboratory, Harvard University, (Nov. 1951).

33. G. Jobst, "Zur Farbentheorie kolloidaler Metallsuspension", Annalen der Physik, 76, pp. 863-888 (1925).

34. E. Kennaugh and R. Sloan, "Quarterly Progress Report 15 June - 15 Sept. 1952 on AF28(099)-90 - Effects of Type of Polarization on Echo Characteristics", The Ohio State University Research Foundation, Report NO. 389-15.

35. M. Kerker, "Scattering Functions for Spherical Particles of Refractive Index of 1.46 - 4.30i", Journal of the Optical Society of America, 45, p. 1081 (1955).

36. D. E. Kerr, Propagation of Short Radio Waves, McGraw-Hill, New York (1951).

37. V. K. LaMer, "Verification of the Mie Theory - Calculations and Measurements of Light Scattered by Dielectric Spherical Particles", OSRD Report 1857 (Sept. 1943).

38. M. P. Langleben and K. L. S. Gunn, "Scattering and Absorption of Microwaves by a Melting Ice Sphere", Scientific Report MW-5, Stormy Weather Research Group, MacDonald Physics Laboratory, McGill University (March 1952).

39. T. Ljunggren, "Contributions to the Theory of Diffraction of Electromagnetic Waves by Spherical Particles", Arkiv fur Matematik Astronomi och Fysik, 36, pp. 1-36 (Oct. 1948).

40. W. Magnus and F. Oberhettinger, Formulas and Theorems for the Functions of Mathematical Physics, Chelsea Publishing Company, New York (1949).

41. G. Mie, "Beiträge zur Optik trüber Medien speziell kolloidaler Metallösungen", Annalen der Physik, 25, pp. 377-445 (1908).

42. National Bureau of Standards, Applied Mathematics, Tables of Scattering Functions for Spherical Particles, Series 4, U.S. Government Printing Office, Washington (1949).

43. National Bureau of Standards, Mathematical Tables Project, Tables of Associated Legendre Functions, Columbia University Press, New York (1945).

44. National Bureau of Standards, Mathematical Tables Project, Tables of Spherical Bessel Functions, Vols. I and II, Columbia University Press, New York (1945).

45. G. R. Paranpje, Y. G. Naik and P. B. Vaidya, "Scattering of Light by Large Water Drops", Part II, Proceedings of the Indian Academy of Science, A9, pp. 352-364 (1939).

46. T. Pearcy and J. M. C. Scott, "The Radar Echoing Power of Conducting Spheres", RRDE , ADRDE Research Report No. 228, (May 1944).

47. R. Penndorf and B. Goldberg, "New Tables of Mie Scattering Functions for Spherical Particles", Air Force Cambridge Research Center, Geophysical Research Paper No. 45, (1956).

48. R. J. Rubenstein and J. R. Pellam, Massachusetts Institute of Technology Laboratory Report No. 42, (April 3, 1943).

49. H. Scharfman, "Scattering from Dielectric Coated Spheres in the Region of First Resonance", Journal of Applied Physics, 25, p. 1352 (1954).

50. H. Scharfman and D. D. King, "Antenna Scattering Measurements by Modulation of the Scatterer", Proceedings of the IRE, 42, 854-858, (May 1954).

51. J. M. C. Scott, "An Asymptotic Series for the Radar Scattering Cross-Section of a Spherical Target", A.E.R.E. T/M 30, A.E.R.E., Harwell (Sept. 1949).

52. Z. Sekera, "Legendre Series of the Scattering Functions for Spherical Particles", Scientific Report No. 5, Air Force Contract AF19(122)-239, University of California at Los Angeles (Nov. 1952).

53. K. M. Siegel, "Bounds on the Legendre Function", Journal of Mathematics and Physics, 24, pp. 43-49 (April 1955).

54. K. M. Siegel, H. A. Alperin, R. R. Bonkowski, J. W. Crispin, A. L. Maffett, C. E. Schensted and I. V. Schensted, "Studies in Radar Cross-Sections VIII - Theoretical Cross-Section as a Function of Separation Angle Between Transmitter and Receiver at Small Wavelengths", Engineering Research Institute, The University of Michigan, Report No. UMM-115, (Oct. 1955).

55. K. M. Siegel, B. H. Gere, I. Marx and F. B. Sleator, "Studies in Radar Cross Sections XI - The Numerical Determination of the Radar Cross-Section of a Prolate Spheroid", Engineering Research Institute, The University of Michigan, Report No. UMM-126, (Dec. 1953).

56. K. M. Siegel, and others, "Studies in Radar Cross-Sections XXI", to be published; also K. M. Siegel, F. V. Schultz, B. H. Gere and F. B. Sleator, "The Theoretical and Numerical Determination of the Radar Cross-Section of a Prolate Spheroid", Proceedings of the Symposium on Electromagnetic Wave Theory, Institute of Radio Engineers Transactions, AP-4 No. 3, (July 1956).

57. W. Spendly, "Scattering by Metallic Spheres", ASRE Ref. XRE (Apr. 4, 1947

58. H. Stenzel, "Über die von einer starren Kugel hervorgerufene Störung des Schallfeldes", Elektrische Nachr. - Tech, 15, pp 71-78, (1938).

59. W. Steubing, "Über die Optischen Eigenschaften kolloidaler Goldlösungen", Annalen der Physik, 26, p. 329, (1908).

60. J. A. Stratton, Electromagnetic Theory, Mc-Graw Hill, New York (1941).

61. C. T. Tai, "On The Theory of Diffraction of Electromagnetic Waves by a Sphere", Technical Report No. 29, SRI Project No. 591, Air Force Contract AF19(604)-266, Stanford Research Institute, (Oct. 1952).

62. _____, "Some Electromagnetic Problems Involving a Sphere", Technical Report No. 41, SRI Project No. 591, Air Force Contract AF19(604)-266. Stanford Research Institute, (April 1953).

63. J. J. Thomson, Recent Researches in Electricity and Magnetism, Oxford, (1893).

64. O. A. Tweitmoe, "Additional Scattering Functions for Spherical Particles", Scientific Report No. 2, Air Force Contract AF19(122)-239, University of California at Los Angeles, (Sept. 1952).

65. H. C. van de Hulst, "Optics of Spherical Particles", Recherches Astronomiques de l'Observatoire d'Utrecht", Amsterdam, (1946).

66. _____, "The Interpretation of Numerical Results Obtained by Rigorous Diffraction Theory for Cylinders and Spheres", Proceeding of the Symposium on Electromagnetic Wave Theory, Institute of Radio Engineers Transactions, AP-4, No. 3, (July 1956).

67. J. R. Wait, "The Radiation Pattern of an Antenna Mounted on a Surface of Large Radius of Curvature", Proceedings of the I.R.E., 44, p. 694, (1956).

68. _____, "Radiation From a Vertical Antenna Over a Curved Stratified Ground", Journal of Research of the National Bureau of Standards, 56, (April 1956).

69. G. N. Watson, "The Diffraction of Electric Waves by the Earth", Proceedings of the Royal Society of London, Series A, 95, pp 83-99, (1918).

70. F. P. White, "The Diffraction of Plane Electromagnetic Waves by a Perfectly Reflecting Sphere", Proceedings of the Royal Society of London, Series A, 100, pp. 505-525 (1922).

71. T. T. Wu, "High Frequency Scattering", Technical Report No. 232, Cruft Laboratory, Harvard University (1956).

72. T. T. Wu and S. I. Rubinow, "The Correction to Geometric Optical Cross-Sections of Circular Cylinders and Spheres", Scientific Report No. 3, Cruft Laboratory, Harvard University, (Sept. 28, 1955).